

Final Report

NASA CR-66904

**OPTIMIZATION STUDY OF A SINGLE
THREE-GIMBALED CONTROL MOMENT GYRO**

By: YASUTADA KASHIWAGI

Prepared for:

NATIONAL AERONAUTICS AND SPACE ADMINISTRATION
LANGLEY RESEARCH CENTER
HAMPTON, VIRGINIA

**CASE FILE
COPY**



STANFORD RESEARCH INSTITUTE
Menlo Park, California 94025 • U.S.A.



STANFORD RESEARCH INSTITUTE
Menlo Park, California 94025 • U.S.A.

Final Report

December 1969

OPTIMIZATION STUDY OF A SINGLE THREE-GIMBALED CONTROL MOMENT GYRO

By: YASUTADA KASHIWAGI

Prepared for:

NATIONAL AERONAUTICS AND SPACE ADMINISTRATION
LANGLEY RESEARCH CENTER
HAMPTON, VIRGINIA

CONTRACT NAS 1-7979

SRI Project 7204

Approved:

DAVID R. BROWN, *Director*
Information Science Laboratory

TORBEN MEISLING, *Executive Director*
Information Science and Engineering Division

Copy No. 2

ABSTRACT

The feasibility study of using a single three-gimbaled control moment gyro is made for fine control of experimental modules attached to an orbital spacecraft.

The suboptimal control laws are derived for the simplified equations, and these control laws performed very well for the original equations. These laws are feedback control laws.

Three optimization problems are considered for the system. These are minimum time control, minimum energy control, and minimization of both time and energy with a weighting factor.

CONTENTS

| | |
|--|-----|
| ABSTRACT. | iii |
| LIST OF ILLUSTRATIONS | vii |
| LIST OF TABLES. | ix |
| LIST OF SYMBOLS | xi |
| I INTRODUCTION AND SUMMARY | 1 |
| A. Introduction. | 1 |
| B. Summary | 2 |
| II CONTROL MOMENT GYRO SYSTEM | 3 |
| III MATHEMATICAL MODEL OF CMG. | 5 |
| A. Preliminary Remarks | 5 |
| B. Equations of Motion | 10 |
| C. Cost Function | 21 |
| IV OPTIMIZATION | 23 |
| A. Simplification. | 23 |
| B. Application of Maximum Principle. | 24 |
| C. Minimum Time Control. | 26 |
| D. Examples of Minimum Time Control. | 30 |
| E. Minimum Power Control | 38 |
| F. Effects of Time Delay | 44 |
| G. Reduction of Model through Polar Coordinates and Another Approach to Time-Optimal Control. | 45 |
| V CONCLUSION | 65 |

APPENDIX--DERIVATION OF FEEDBACK CONTROL FOR
THREE-DIMENSIONAL SYSTEM. 67

REFERENCES. 75

ILLUSTRATIONS

| | | |
|-----------|--|----|
| Figure 1 | Sketch of CMG. | 7 |
| Figure 2 | Behavior of θ_x | 31 |
| Figure 3 | $I_{\dot{\theta}_x} = \bar{M}_x$; $\bar{M}_x = 10 \sin(\pi t)$ ft-lb (0.5 c/s). | 33 |
| Figure 4 | $I_{\dot{\theta}_x} = \bar{M}_x$; $\bar{M}_x = 10 \sin(4\pi t)$ ft-lb (2 c/s) | 34 |
| Figure 5 | $I_{\dot{\theta}_x} = \bar{M}_x$; $\bar{M}_x = 10 \sin(10\pi t)$ ft-lb (5 c/s). | 35 |
| Figure 6 | Suboptimal Trajectories (x_1 - x_2 plane). | 36 |
| Figure 7 | Suboptimal Trajectories (x_3 - x_4 plane). | 37 |
| Figure 8 | Behavior of Gimbals; $\bar{M}_x = 25$ ft-lb (Step Input) | 39 |
| Figure 9 | Behavior of Gimbals; $\bar{M}_x = 10 \sin(\pi t)$ ft-lb (0.5 c/s). | 40 |
| Figure 10 | Behavior of Gimbals. | 41 |
| Figure 11 | Illustration of \bar{u}_1 | 44 |
| Figure 12 | Optimal Trajectories in p-r- ψ Space Projected Onto the p-r Plane | 58 |
| Figure 13 | The Pattern of Optimal Trajectories in p-r- ψ Space Projected Onto the p-r Plane | 59 |
| Figure 14 | Comparison of Optimal and Feedback Trajectories in p-r Plane for Initial Point A. | 60 |
| Figure 15 | Feedback Trajectory in z_1 - z_2 Plane for Initial Point A. | 61 |
| Figure 16 | Comparison of Optimal and Feedback Trajectories in p-r Plane for Initial Point B. | 62 |

| | | |
|------------|--|-----|
| Figure 17 | Feedback Trajectory in z_1-z_2 Plane for Initial Point B. | 63 |
| Figure A-1 | Flow Chart Used for Obtaining Figures 14-17. . | 71. |

TABLES

| | | |
|-----------|---|----|
| Table I | Maximum Deviation of θ_y | 32 |
| Table II | Comparison of Time Requirement | 38 |
| Table A-1 | A Provisional Suboptimal Feedback Control Law. | 70 |
| Table A-2 | Suggested Feedback Control for Use with Eqs. (87), (88), and (92) when $r \neq s$ and $\eta \neq 0$ | 73 |

SYMBOLS

| | |
|--------------------|---|
| a, b | Real constant |
| G, G_i | Moment |
| H | Angular momentum of the rotor |
| \mathcal{H} | Hamiltonian function |
| I_{ij} | Moment of inertia of the gimbals |
| \tilde{I}_i | Principal moment of inertia of the rotor |
| I_x, I_y, I_z | Moment of inertia of the platform |
| J, J_1, J_2, J_3 | Cost functions |
| k, \bar{k} | Weighting parameters |
| L, K | Real constants |
| M_x, M_y, M_z | Moment about x, y, z axes, respectively |
| M | Vector whose elements are M_x, M_y, M_z |
| \bar{M}_x | Forcing term |
| p, r, s | Polar coordinate radii |
| S | Laplace transform variable |
| t | Time |
| T_1, T_2, T_3 | Torque produced by CMG |
| T | Vector whose elements are T_1, T_2, T_3 |
| u_1, u_2, u_3 | Control variable |
| w_i, v_i | Transformed control variables |

| | |
|---|--|
| W_1, W_2 | Real variable |
| x_i, y_i, z_i | Dependent variable |
| α | Control magnitude (proportional to maximum rate for inner two gimbals) |
| $\bar{\alpha}, \beta$ | Real constant |
| δ | Real constant |
| ϵ_1, ϵ_2 | Real variable or constant |
| $\theta_x, \theta_y, \theta_z$ | Angular deviation of the platform |
| θ^* | Vector whose elements are $\theta_x, \theta_y, \theta_z$ |
| $\theta_1, \theta_2, \theta_3$ | Angular deviation of the gimbals |
| θ | Vector whose elements are $\theta_1, \theta_2, \theta_3$ |
| λ_i | Adjoint variable |
| ψ, η | Angles used in polar coordinate model |
| τ | Time ($\tau = t_f - t$) |
| φ, Θ, σ | Polar coordinate angles |
| $\omega_i, \omega_{ij}, \tilde{\omega}$ | Angular velocity |

I INTRODUCTION AND SUMMARY

A. Introduction

This report is concerned with the feasibility of using a single three-gimbaled control moment gyro for fine control of experimental modules attached to an orbital spacecraft.

The prototype space vehicle considered by NASA consists primarily of an orbital workshop, a command service module, and several experimental modules. A system of three double-gimbaled control moment gyros (CMG's) is designed to control the attitude of the orbital workshop.^{1*} Since the orbital workshop and the other modules are not rigidly connected, the other modules can be considered as masses connected by springs; it is thus improbable that the present CMG system can provide accurate attitude control for the attached modules.

Additional control of the experimental modules could be provided by a single three-gimbaled CMG.

Control moment gyros have many attractive advantages--among them high accuracy and sufficiently low power requirements that the gyro can be operated from energy supplied by solar panels or from fuel cells. Further, since CMG's do not produce gases around the space vehicle, they do not interfere with optical experiments. These advantages indicate that CMG's are the logical choice for the next generation of attitude controllers for space vehicles and experimental modules.

* References are listed at the end of the report.

B. Summary

A theoretical study has been made for a single three-gimbaled control moment gyro. Three optimization problems, namely, minimum time, minimum energy, and the minimization of both time and energy with a weighting factor, are considered.

In order to obtain a feasible feedback control law, the equations of motion are simplified. The suboptimal control derived for the simplified equations performed very well for the original equations.

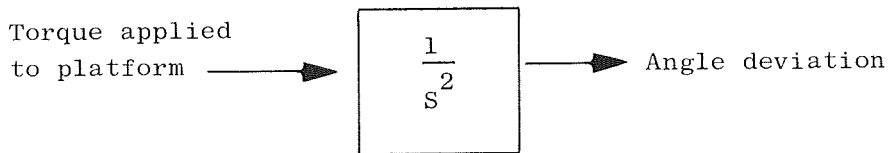
The outer gimbal is designed for controlling the disturbances about the Z-axis. However, the analysis shows that a significant improvement in the outer gimbal configurations is required in order to use the outer gimbal for controlling the disturbances about the Z-axis. It is important to note that the outer gimbal in the present form permits a wider range of X and Y axis control.

It is found that the optimal control law that minimizes both time and energy with a weighting factor can be constructed by adding a dead zone to the time-optimal switching curves. The width of the dead band is a function of the weighting factor.

II CONTROL MOMENT GYRO SYSTEM

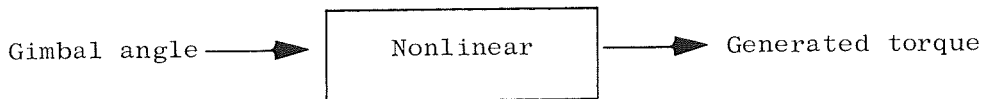
In order to find the optimal control law, the total system is divided into two parts, namely, the controlled part (platform) and the control element (CMG), indicated schematically below:

$$M = \begin{bmatrix} M_x \\ M_y \\ M_z \end{bmatrix} \quad \theta^* = \begin{bmatrix} \theta_x \\ \theta_y \\ \theta_z \end{bmatrix}$$



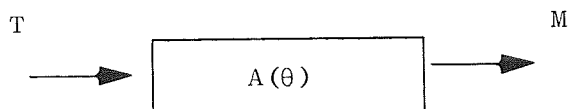
Controlled Part (Platform)

$$\theta = \begin{bmatrix} \theta_1 \\ \theta_2 \\ \theta_3 \end{bmatrix} \quad T = \begin{bmatrix} T_1 \\ T_2 \\ T_3 \end{bmatrix}$$



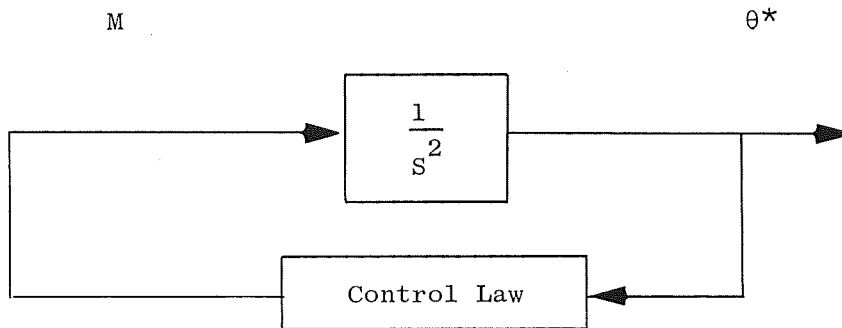
Control Element (CMG)

The values of T and M are related as follows:



The three optimization problems, namely, time optimal, minimum energy, and the minimization of the combination of energy and time, are considered in this report. General comments for the three problems are given below.

Time-Optimal Control--The time-optimal-control law is found by considering only the controlled part:



Once the time-optimal-control law $M(\theta^*)$ is determined, the unique solution $\theta(\theta^*)$ from the equation describing the control element is also determined.

Minimum-Energy Control--If the problem is defined as that of minimizing the energy consumption without having any limitation in time, then the solution is trivial. The answer is to use almost no energy and to consume infinite time.

Minimization of the Combination of Energy and Time--The main problem in this research is to find the control law that minimizes the combination of energy consumption and time with a weighting factor. The non-linearity in the equation of motion of a CMG causes the difficulty in finding the feedback optimal control law. When the implementation of the solution is considered, it is better to have a feedback control law for a simplified model than a time-dependent solution for the original equation with a high degree of nonlinearity. The simplification of the equation is discussed in Section III.

III MATHEMATICAL MODEL OF CMG

A. Preliminary Remarks

It is necessary to define the torques, angular velocities, and angular momentum before describing the equation of motion.

If \underline{n}_i ($i = 1, 2, 3$) is a right-handed set of mutually perpendicular principal directions of a rigid body R for the mass center \underline{P}^* of R, and if these unit vectors are fixed in R, then the torque $\underline{T}^{R'}{}^R$ of the inertia couple acting on R in a reference frame R' is given by²

$$\begin{aligned} \underline{T}^{R'}{}^R = & - \left[I_1 \frac{d \omega_1^{R'}{}^R}{dt} - (I_2 - I_3) \omega_2^{R'}{}^R \omega_3^{R'}{}^R \right] \underline{n}_1 \\ & - \left[I_2 \frac{d \omega_2^{R'}{}^R}{dt} - (I_3 - I_1) \omega_3^{R'}{}^R \omega_1^{R'}{}^R \right] \underline{n}_2 \\ & - \left[I_3 \frac{d \omega_3^{R'}{}^R}{dt} - (I_1 - I_2) \omega_1^{R'}{}^R \omega_2^{R'}{}^R \right] \underline{n}_3 \quad , \quad (1) \end{aligned}$$

where $\omega_i^{R'}{}^R$ is the \underline{n}_i measure number of the angular velocity of R in R' and I_i is the principal moment of inertia of R for \underline{P}^* .

Define the moment of inertia of three gimbals--namely, inner, middle, and outer--as follows:

$$[I]_i = \begin{bmatrix} I_{1i} & 0 & 0 \\ 0 & I_{2i} & 0 \\ 0 & 0 & I_{3i} \end{bmatrix} \quad , \quad i = 1, 2, 3 \quad .$$

The first subscripts indicate the axes (x, y, z) and the second subscripts indicate the reference frames (inner gimbal, middle gimbal, outer gimbal).*

Define the angular velocities of those gimbals and their time derivatives with respect to the main body as

$$\{\omega\}_i = \begin{Bmatrix} \omega_{1i} \\ \omega_{2i} \\ \omega_{3i} \end{Bmatrix}, \quad \{\dot{\omega}\}_i = \begin{Bmatrix} \dot{\omega}_{1i} \\ \dot{\omega}_{2i} \\ \dot{\omega}_{3i} \end{Bmatrix}, \quad i = 1, 2, 3,$$

and also define the matrix $[\omega]_i$ as

$$[\omega]_i = \begin{bmatrix} 0 & -\omega_{3i} & \omega_{2i} \\ \omega_{3i} & 0 & -\omega_{1i} \\ -\omega_{2i} & \omega_{1i} & 0 \end{bmatrix}, \quad i = 1, 2, 3.$$

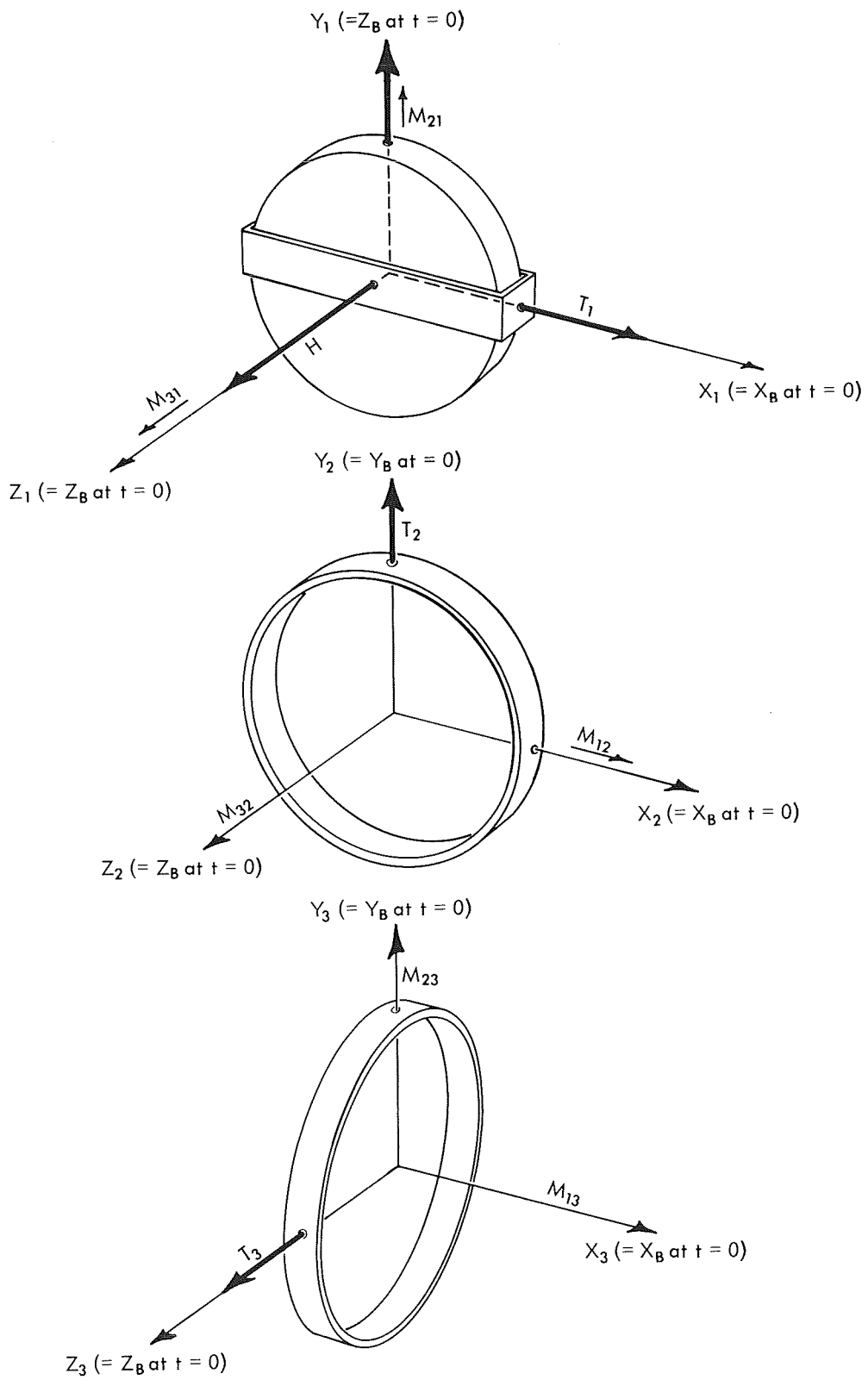
Then the torque $\{T\}_i$ of the inertia couple acting on a gimbal i in a reference frame B, main body [refer to Eq. (1)], is described as

$$\{T\}_i = \underline{\underline{B}}_T^i = - [I]_i \{\dot{\omega}\}_i - [\omega]_i [I]_i \{\omega\}_i, \quad i = 1, 2, 3. \quad (2)$$

The angular momentum $\underline{\underline{H}}$ of the rotor relative to the mass center in B is expressed as

$$\underline{\underline{H}} = \tilde{I}_1 \omega_{11} \underline{\underline{n}}_1 + \tilde{I}_2 \omega_{22} \underline{\underline{n}}_2 + \tilde{I}_3 (\omega_{33} + \tilde{\omega}) \underline{\underline{n}}_3,$$

* Refer to Figure 1.



TA-7204-1

FIGURE 1 SKETCH OF CMG

where \tilde{I}_1 is the principal moment of inertia of the rotor for the mass center, $\tilde{\omega}$ is the angular velocity of the rotor with respect to the inner gimbal, and as previously defined \underline{n}_1 , \underline{n}_2 , and \underline{n}_3 are mutually perpendicular unit vectors fixed in the inner gimbal. In this case, a rigid body R corresponds to the inner gimbal. The sum of the moments about the mass center of the rotor of all gravitational and contact forces acting on the rotor is related to the angular momentum \underline{H} as follows:

$$\begin{aligned} \underline{G} &= \frac{B}{dt} \underline{H} = \frac{1}{dt} \underline{H} + \underline{B} \underline{\omega} \times \underline{H} \\ &= \tilde{I}_1 \dot{\omega}_{11} \underline{n}_1 + \tilde{I}_2 \dot{\omega}_{22} \underline{n}_2 + \tilde{I}_3 \dot{\omega}_{33} \underline{n}_3 \\ &\quad + \begin{vmatrix} \underline{n}_1 & \underline{n}_2 & \underline{n}_3 \\ \omega_{11} & \omega_{21} & \omega_{31} \\ \tilde{I}_1 \omega_{11} & \tilde{I}_2 \omega_{22} & \tilde{I}_3 (\omega_{33} + \tilde{\omega}) \end{vmatrix} \\ &= \left. \begin{matrix} \tilde{I}_1 \dot{\omega}_{11} - \tilde{I}_2 \omega_{31} \omega_{22} + \tilde{I}_3 \omega_{21} (\omega_{33} + \tilde{\omega}) \\ \tilde{I}_2 \dot{\omega}_{22} + \tilde{I}_1 \omega_{31} \omega_{11} - \tilde{I}_3 \omega_{11} (\omega_{33} + \tilde{\omega}) \\ \tilde{I}_3 \dot{\omega}_{33} - \tilde{I}_1 \omega_{21} \omega_{11} + \tilde{I}_2 \omega_{11} \omega_{22} \end{matrix} \right\}_1 \end{aligned}$$

If $\tilde{\omega} \gg \omega_{ij}$ and $\tilde{\omega} \gg \dot{\omega}_{ii}$, then

$$\underline{G} = \begin{Bmatrix} G_1 \\ G_2 \\ G_3 \end{Bmatrix}_1 \cong \begin{Bmatrix} \omega_{21} H \\ -\omega_{11} H \\ 0 \end{Bmatrix}_1, \quad (3)$$

where $H = \tilde{I}_3 \tilde{\omega}$.

Let us define the coordinate transformation matrices as follows:

(1) Rotation θ_3 about z_3 axis

$$\begin{Bmatrix} x_3 \\ y_3 \\ z_3 \end{Bmatrix} = [A]_3 \begin{Bmatrix} x_B \\ y_B \\ z_B \end{Bmatrix},$$

where

$$[A]_3 = \begin{bmatrix} \cos \theta_3 & \sin \theta_3 & 0 \\ -\sin \theta_3 & \cos \theta_3 & 0 \\ 0 & 0 & 1 \end{bmatrix},$$

(2) Rotation θ_2 about y_2 axis

$$\begin{Bmatrix} x_2 \\ y_2 \\ z_2 \end{Bmatrix} = [A]_2 \begin{Bmatrix} x_3 \\ y_3 \\ z_3 \end{Bmatrix},$$

where

$$[A]_2 = \begin{bmatrix} \cos \theta_2 & 0 & -\sin \theta_2 \\ 0 & 1 & 0 \\ \sin \theta_2 & 0 & \cos \theta_2 \end{bmatrix},$$

(3) Rotation θ_1 about x_1 axis

$$\begin{Bmatrix} x_1 \\ y_1 \\ z_1 \end{Bmatrix} = [A]_1 \begin{Bmatrix} x_2 \\ y_2 \\ z_2 \end{Bmatrix},$$

where

$$[A]_1 = \begin{bmatrix} 1 & 0 & 0 \\ 0 & \cos \theta_1 & \sin \theta_1 \\ 0 & -\sin \theta_1 & \cos \theta_1 \end{bmatrix}.$$

B. Equations of Motion

The equation of motion of the inner gimbal is described as

$$\begin{Bmatrix} T_1 \\ M_{21} \\ M_{31} \end{Bmatrix} + \begin{Bmatrix} G_1 \\ G_2 \\ G_3 \end{Bmatrix}_1 + \{T\}_1 = 0 \quad (4)$$

The first term represents the torque acting on the inner gimbal, the second term represents the precession torque, and the third term represents the torque of the inertia couple acting on the inner gimbal.

Similarly, equations for the middle and outer gimbals are expressed as

$$\begin{Bmatrix} M_{12} \\ T_2 \\ M_{32} \end{Bmatrix} - [A]_1^T \begin{Bmatrix} T_1 \\ M_{21} \\ M_{31} \end{Bmatrix} + \{T\}_2 = 0, \quad (5)$$

$$\begin{Bmatrix} M_{13} \\ M_{23} \\ T_3 \end{Bmatrix} - [A]_2^T \begin{Bmatrix} M_{12} \\ T_2 \\ M_{32} \end{Bmatrix} + \{T\}_3 = 0 \quad . \quad (6)$$

Substituting Eq. (2) into Eqs. (4), (5), and (6) yields

$$\begin{Bmatrix} T_1 \\ M_{21} \\ M_{31} \end{Bmatrix} = - \begin{Bmatrix} G_1 \\ G_2 \\ G_3 \end{Bmatrix}_1 + [I]_1 \{\dot{\phi}\}_1 + [\omega]_1 [I]_1 \{\omega\}_1 \quad ,$$

$$\begin{Bmatrix} M_{12} \\ T_2 \\ M_{32} \end{Bmatrix} = [A]_1^T \begin{Bmatrix} T_1 \\ M_{21} \\ M_{31} \end{Bmatrix} + [I]_2 \{\dot{\omega}\}_2 + [\omega]_2 [I]_2 \{\omega\}_2 \quad ,$$

and

$$\begin{Bmatrix} M_{13} \\ M_{23} \\ T_3 \end{Bmatrix} = [A]_2^T \begin{Bmatrix} M_{12} \\ T_2 \\ M_{32} \end{Bmatrix} + [I]_3 \{\dot{\omega}\}_3 + [\omega]_3 [I]_3 \{\omega\}_3 \quad .$$

Hence, we have

$$\begin{Bmatrix} T_1 \\ M_{21} \\ M_{31} \end{Bmatrix} = \begin{Bmatrix} -\omega_{21} & H \\ \omega_{11} & H \\ 0 \end{Bmatrix} + \begin{Bmatrix} I_{11} \dot{\omega}_{11} - (I_{21} - I_{31}) \omega_{21} \omega_{31} \\ I_{21} \dot{\omega}_{21} - (I_{31} - I_{11}) \omega_{31} \omega_{11} \\ I_{31} \dot{\omega}_{31} - (I_{11} - I_{21}) \omega_{11} \omega_{21} \end{Bmatrix} \quad (7)$$

$$\begin{Bmatrix} M_{12} \\ T_2 \\ M_{32} \end{Bmatrix} = \begin{bmatrix} 1 & 0 & 0 \\ 0 & \cos \theta_1 & -\sin \theta_1 \\ 0 & \sin \theta_1 & \cos \theta_1 \end{bmatrix} \begin{Bmatrix} I_{11} \dot{\psi}_{11} - (I_{21} - I_{31}) \omega_{21} \omega_{31} - \omega_{21}^H \\ I_{21} \dot{\psi}_{21} - (I_{31} - I_{11}) \omega_{31} \omega_{11} + \omega_{11}^H \\ I_{31} \dot{\psi}_{31} - (I_{11} - I_{21}) \omega_{11} \omega_{21} \end{Bmatrix} \\ + \begin{Bmatrix} I_{12} \dot{\psi}_{12} - (I_{22} - I_{32}) \omega_{22} \omega_{32} \\ I_{22} \dot{\psi}_{22} - (I_{32} - I_{12}) \omega_{32} \omega_{12} \\ I_{32} \dot{\psi}_{32} - (I_{12} - I_{22}) \omega_{12} \omega_{22} \end{Bmatrix} \quad (8)$$

$$\begin{Bmatrix} M_{13} \\ M_{23} \\ T_3 \end{Bmatrix} = \begin{bmatrix} \cos \theta_2 & 0 & \sin \theta_2 \\ 0 & 1 & 0 \\ -\sin \theta_2 & 0 & \cos \theta_2 \end{bmatrix} \begin{bmatrix} 1 & 0 & 0 \\ 0 & \cos \theta_1 & -\sin \theta_1 \\ 0 & \sin \theta_1 & \cos \theta_1 \end{bmatrix} \\ \times \begin{Bmatrix} I_{11} \dot{\psi}_{11} - (I_{21} - I_{31}) \omega_{21} \omega_{31} - \omega_{21}^H \\ I_{21} \dot{\psi}_{21} - (I_{31} - I_{11}) \omega_{31} \omega_{11} + \omega_{11}^H \\ I_{31} \dot{\psi}_{31} - (I_{11} - I_{21}) \omega_{11} \omega_{21} \end{Bmatrix} \\ + \begin{bmatrix} \cos \theta_2 & 0 & \sin \theta_2 \\ 0 & 1 & 0 \\ -\sin \theta_2 & 0 & \cos \theta_2 \end{bmatrix} \begin{Bmatrix} I_{12} \dot{\psi}_{12} - (I_{22} - I_{32}) \omega_{22} \omega_{32} \\ I_{22} \dot{\psi}_{22} - (I_{32} - I_{12}) \omega_{32} \omega_{12} \\ I_{32} \dot{\psi}_{32} - (I_{12} - I_{22}) \omega_{12} \omega_{22} \end{Bmatrix}$$

$$+ \begin{Bmatrix} I_{13} \dot{\psi}_{13} - (I_{23} - I_{33}) \omega_{23} \omega_{33} \\ I_{23} \dot{\psi}_{23} - (I_{33} - I_{13}) \omega_{33} \omega_{13} \\ I_{33} \dot{\psi}_{33} - (I_{13} - I_{23}) \omega_{13} \omega_{23} \end{Bmatrix} \quad (9)$$

The elements of $\{\omega\}_i$ and $\{\dot{\omega}\}_i$ are expressed in terms of θ_i and $\dot{\theta}_i$ as follows:

$$\begin{Bmatrix} \omega_{13} \\ \omega_{23} \\ \omega_{33} \end{Bmatrix} = \{\omega\}_3 = \underline{B}_{\omega}^3 = \begin{Bmatrix} 0 \\ 0 \\ \dot{\theta}_3 \end{Bmatrix},$$

$$\begin{Bmatrix} \omega_{12} \\ \omega_{22} \\ \omega_{32} \end{Bmatrix} = \{\omega\}_2 = \underline{B}_{\omega}^2 = \underline{3}_{\omega}^2 + \underline{B}_{\omega}^3 = \begin{Bmatrix} -\dot{\theta}_3 \sin \theta_2 \\ \dot{\theta}_2 \\ \dot{\theta}_3 \cos \theta_2 \end{Bmatrix},$$

$$\begin{Bmatrix} \omega_{11} \\ \omega_{21} \\ \omega_{31} \end{Bmatrix} = \{\omega\}_1 = \underline{B}_{\omega}^1 = \underline{2}_{\omega}^1 + \underline{B}_{\omega}^2 = \begin{Bmatrix} \dot{\theta}_1 - \dot{\theta}_3 \sin \theta_2 \\ \dot{\theta}_2 \cos \theta_1 + \dot{\theta}_3 \sin \theta_1 \cos \theta_2 \\ -\dot{\theta}_2 \sin \theta_1 + \dot{\theta}_3 \cos \theta_1 \cos \theta_2 \end{Bmatrix}$$

$$\begin{Bmatrix} \dot{\omega}_{13} \\ \dot{\omega}_{23} \\ \dot{\omega}_{33} \end{Bmatrix} = \{\dot{\omega}\}_3 = \frac{B_d B_{\omega}^3}{dt} = \begin{Bmatrix} 0 \\ 0 \\ \ddot{\theta}_3 \end{Bmatrix},$$

$$\begin{Bmatrix} \dot{\omega}_{12} \\ \dot{\omega}_{22} \\ \dot{\omega}_{32} \end{Bmatrix} = \{\dot{\omega}\}_2 = \frac{B_d B_{\omega}^2}{dt} = \begin{Bmatrix} -\ddot{\theta}_3 \sin \theta_2 - \dot{\theta}_3 \dot{\theta}_2 \cos \theta_2 \\ \ddot{\theta}_2 \\ \ddot{\theta}_3 \cos \theta_2 - \dot{\theta}_3 \dot{\theta}_2 \sin \theta_2 \end{Bmatrix},$$

$$\begin{Bmatrix} \dot{\omega}_{11} \\ \dot{\omega}_{21} \\ \dot{\omega}_{31} \end{Bmatrix} = \{\dot{\omega}\}_1 = \frac{B_d B_{\omega}^1}{dt}$$

$$= \begin{Bmatrix} \ddot{\theta}_1 - \ddot{\theta}_3 \sin \theta_2 - \dot{\theta}_3 \dot{\theta}_2 \cos \theta_2 \\ \ddot{\theta}_2 \cos \theta_1 - \dot{\theta}_2 \dot{\theta}_1 \sin \theta_1 + \ddot{\theta}_3 \sin \theta_1 \cos \theta_2 - \dot{\theta}_3 (\dot{\theta}_2 \sin \theta_1 \sin \theta_2 - \dot{\theta}_1 \cos \theta_1 \cos \theta_2) \\ -\ddot{\theta}_2 \sin \theta_1 - \dot{\theta}_2 \dot{\theta}_1 \cos \theta_1 + \ddot{\theta}_3 \cos \theta_1 \cos \theta_2 - \dot{\theta}_3 (\dot{\theta}_1 \sin \theta_1 \cos \theta_2 + \dot{\theta}_2 \cos \theta_1 \sin \theta_2) \end{Bmatrix}.$$

Substituting these values into Eqs. (7), (8), and (9) results in the following:

$$\begin{aligned}
T_1 = & I_{11}(\ddot{\theta}_1 - \ddot{\theta}_3 \sin\theta_2 - \dot{\theta}_3 \dot{\theta}_2 \cos\theta_2) \\
& - (I_{21} - I_{31})(\dot{\theta}_2 \cos\theta_1 + \dot{\theta}_3 \sin\theta_1 \cos\theta_2)(-\dot{\theta}_2 \sin\theta_1 + \dot{\theta}_3 \cos\theta_1 \cos\theta_2) \\
& - H(\dot{\theta}_2 \cos\theta_1 + \dot{\theta}_3 \sin\theta_1 \cos\theta_2) \tag{10}
\end{aligned}$$

$$\begin{aligned}
T_2 = & \cos\theta_1 \left[I_{21} \left\{ \ddot{\theta}_2 \cos\theta_1 - \dot{\theta}_2 \dot{\theta}_1 \sin\theta_1 + \ddot{\theta}_3 \sin\theta_1 \cos\theta_2 \right. \right. \\
& \left. \left. - \dot{\theta}_3 (\dot{\theta}_2 \sin\theta_1 \sin\theta_2 - \dot{\theta}_1 \cos\theta_1 \cos\theta_2) \right\} \right. \\
& \left. - (I_{31} - I_{11})(-\dot{\theta}_2 \sin\theta_1 + \dot{\theta}_3 \cos\theta_1 \cos\theta_2)(\dot{\theta}_1 - \dot{\theta}_3 \sin\theta_2) \right. \\
& \left. + (\dot{\theta}_1 - \dot{\theta}_3 \sin\theta_2) H \right] \\
& - \sin\theta_1 \left[I_{31} \left\{ -\ddot{\theta}_2 \sin\theta_1 - \dot{\theta}_2 \dot{\theta}_1 \cos\theta_1 + \ddot{\theta}_3 \cos\theta_1 \cos\theta_2 \right. \right. \\
& \left. \left. - \dot{\theta}_3 (\dot{\theta}_1 \sin\theta_1 \cos\theta_2 + \dot{\theta}_2 \cos\theta_1 \sin\theta_2) \right\} \right. \\
& \left. - (I_{11} - I_{21})(\dot{\theta}_1 - \dot{\theta}_3 \sin\theta_2)(\dot{\theta}_2 \cos\theta_1 + \dot{\theta}_3 \sin\theta_1 \cos\theta_2) \right] \\
& + I_{22} \ddot{\theta}_2 + (I_{32} - I_{12})(\dot{\theta}_3)^2 \cos\theta_2 \sin\theta_2 \tag{11}
\end{aligned}$$

$$\begin{aligned}
T_3 = & -I_{11}(\ddot{\theta}_1 - \ddot{\theta}_3 \sin\theta_2 - \dot{\theta}_3 \dot{\theta}_2 \cos\theta_2) \sin\theta_2 \\
& + (I_{21} - I_{31}) (\dot{\theta}_2 \cos\theta_1 + \dot{\theta}_3 \cos\theta_2 \sin\theta_1) (-\dot{\theta}_2 \sin\theta_1 + \dot{\theta}_3 \cos\theta_1 \cos\theta_2) \sin\theta_2 \\
& + (\dot{\theta}_2 \cos\theta_1 + \dot{\theta}_3 \sin\theta_1 \cos\theta_2) \cdot H \sin\theta_2 \\
& + I_{21} \left\{ \ddot{\theta}_2 \cos\theta_1 - \dot{\theta}_2 \dot{\theta}_1 \sin\theta_1 + \ddot{\theta}_3 \sin\theta_1 \cos\theta_2 \right. \\
& \quad \left. - \dot{\theta}_3 (\dot{\theta}_2 \sin\theta_1 \sin\theta_2 - \dot{\theta}_1 \cos\theta_1 \cos\theta_2) \right\} \sin\theta_1 \cos\theta_2 \\
& - (I_{31} - I_{11}) (-\dot{\theta}_2 \sin\theta_1 + \dot{\theta}_3 \cos\theta_1 \cos\theta_2) (\dot{\theta}_1 - \dot{\theta}_3 \sin\theta_2) \sin\theta_1 \cos\theta_2 \\
& + (\dot{\theta}_1 - \dot{\theta}_3 \sin\theta_2) H \sin\theta_1 \cos\theta_2 \\
& + I_{31} \left\{ -\ddot{\theta}_2 \sin\theta_1 - \dot{\theta}_2 \dot{\theta}_1 \cos\theta_1 + \ddot{\theta}_3 \cos\theta_1 \cos\theta_2 \right. \\
& \quad \left. - \dot{\theta}_3 (\dot{\theta}_1 \sin\theta_1 \cos\theta_2 + \dot{\theta}_2 \cos\theta_1 \sin\theta_2) \right\} \cos\theta_1 \cos\theta_2 \\
& - (I_{11} - I_{21}) (\dot{\theta}_1 - \dot{\theta}_3 \sin\theta_2) (\ddot{\theta}_2 \cos\theta_1 + \dot{\theta}_3 \sin\theta_1 \cos\theta_2) \\
& - I_{12} (-\ddot{\theta}_3 \sin\theta_2 - \dot{\theta}_3 \dot{\theta}_2 \cos\theta_2) \sin\theta_2 \\
& + (I_{22} - I_{32}) \dot{\theta}_2 \dot{\theta}_3 \sin\theta_2 \cos\theta_2 + I_{32} (\ddot{\theta}_3 \cos\theta_2 - \dot{\theta}_3 \dot{\theta}_2 \sin\theta_2) \cos\theta_2 \\
& - (I_{22} - I_{12}) \dot{\theta}_2 \dot{\theta}_3 \sin\theta_2 \cos\theta_2 + I_{33} \ddot{\theta}_3 \quad . \tag{12}
\end{aligned}$$

If $\sin \theta_i \approx \theta_i$ and $\cos \theta_i \approx 1$ ($i = 1, 2$), then the equations described above will be simplified as follows:

$$\begin{aligned}
T_1 = & I_{11}(\ddot{\theta}_1 - \ddot{\theta}_3\theta_2 - \dot{\theta}_3\dot{\theta}_2) - (I_{21} - I_{31})(\dot{\theta}_2 + \dot{\theta}_3\theta_1)(-\dot{\theta}_2\theta_1 + \dot{\theta}_3) \\
& - H(\dot{\theta}_2 + \dot{\theta}_3\theta_1) \quad , \tag{13}
\end{aligned}$$

$$\begin{aligned}
T_2 = & I_{21}\{\ddot{\theta}_2 - \dot{\theta}_2\dot{\theta}_1\theta_1 + \ddot{\theta}_3\theta_1 - \dot{\theta}_3(\dot{\theta}_2\theta_1\theta_2 - \dot{\theta}_1)\} \\
& - (I_{31} - I_{11})(-\dot{\theta}_2\theta_1 + \dot{\theta}_3)(\dot{\theta}_1 - \dot{\theta}_3\theta_2) + H(\dot{\theta}_1 - \dot{\theta}_3\theta_2) \\
& - I_{31}\theta_1\{-\ddot{\theta}_2\theta_1 - \dot{\theta}_2\dot{\theta}_1 + \ddot{\theta}_3 - \dot{\theta}_3(\dot{\theta}_1\theta_1 + \dot{\theta}_2\theta_2)\} \\
& - (I_{11} - I_{21})(\dot{\theta}_1 - \dot{\theta}_3\theta_2)(\dot{\theta}_2 + \dot{\theta}_3\theta_1) \\
& + I_{22}\ddot{\theta}_2 + (I_{32} - I_{12})\dot{\theta}_3^2\theta_2 \quad , \tag{14}
\end{aligned}$$

$$\begin{aligned}
T_3 = & -I_{11}(\ddot{\theta}_1 - \ddot{\theta}_3\theta_2 - \dot{\theta}_3\dot{\theta}_2)\theta_2 \\
& + (I_{21} - I_{31})(\dot{\theta}_2 + \dot{\theta}_3\theta_1)(-\dot{\theta}_2\theta_1 + \dot{\theta}_3)\theta_2 + H\theta_2(\dot{\theta}_2 + \dot{\theta}_3\theta_1) \\
& + I_{21}\theta_1\{\ddot{\theta}_2 - \dot{\theta}_2\dot{\theta}_1\theta_1 + \ddot{\theta}_3\theta_1 - \dot{\theta}_3(\dot{\theta}_2\theta_1\theta_2 - \dot{\theta}_1)\} \\
& - (I_{31} - I_{11})\theta_1(-\dot{\theta}_2\theta_1 + \dot{\theta}_3)(\dot{\theta}_1 - \dot{\theta}_3\theta_2) + H\theta_1(\dot{\theta}_1 - \dot{\theta}_3\theta_2) \\
& + I_{31}\{-\ddot{\theta}_2\theta_1 - \dot{\theta}_2\dot{\theta}_1 + \ddot{\theta}_3 - \dot{\theta}_3(\dot{\theta}_1\theta_1 + \dot{\theta}_2\theta_2)\} \\
& - (I_{11} - I_{21})(\dot{\theta}_1 - \dot{\theta}_3\theta_2)(\dot{\theta}_2 + \dot{\theta}_3\theta_1) - I_{12}(-\ddot{\theta}_3\theta_2 - \dot{\theta}_3\dot{\theta}_2)\theta_2 \\
& + (I_{22} - I_{32})\dot{\theta}_2\dot{\theta}_3\theta_2 + I_{32}(\ddot{\theta}_3 - \dot{\theta}_3\dot{\theta}_2\theta_2) \\
& - (I_{22} - I_{12})\dot{\theta}_2\dot{\theta}_3\theta_2 + I_{33}\ddot{\theta}_3 \quad . \tag{15}
\end{aligned}$$

The data given by NASA are $H = 1000$ ft-lb-second,

$$I_1 = \begin{bmatrix} 1 & 0 & 0 \\ 0 & 1 & 0 \\ 0 & 0 & 1 \end{bmatrix} \text{ slg-ft}^2, \quad I_2 = \begin{bmatrix} 1 & 0 & 0 \\ 0 & 4 & 0 \\ 0 & 0 & 4 \end{bmatrix} \text{ slg-ft}^2, \quad \text{and}$$

$$I_3 = \begin{bmatrix} 10 & 0 & 0 \\ 0 & 6 & 0 \\ 0 & 0 & 8 \end{bmatrix} \text{ slg-ft}^2.$$

Hence, if $I_{11} = I_{21} = I_{31}$ and $I_{12} = kI_{22} = kI_{32}$ ($k < 1$), then the three equations will become

$$T_1 = I_{11}(\ddot{\theta}_1 - \ddot{\theta}_3\theta_2 - \dot{\theta}_3\dot{\theta}_2) - H(\dot{\theta}_2 + \dot{\theta}_3\theta_1), \quad (16)$$

$$T_2 = I_{11}\left\{\ddot{\theta}_2(1 + \theta_1^2) + \dot{\theta}_3\dot{\theta}_1(1 + \theta_1^2) - \dot{\theta}_3^2\theta_2\right\} \\ + I_{22}(\ddot{\theta}_2 + \dot{\theta}_3^2\theta_2) + H(\dot{\theta}_1 - \dot{\theta}_3\theta_2), \quad (17)$$

$$T_3 = -I_{11}\left\{\ddot{\theta}_1\theta_2 - \ddot{\theta}_3(1 + \theta_1^2 + \theta_2^2) + \dot{\theta}_1\dot{\theta}_2(1 + \theta_1^2) + \dot{\theta}_2\dot{\theta}_3\theta_1^2\theta_2\right\} \\ + I_{22}\left\{\ddot{\theta}_3(1 + k\theta_2^2) - 2(1 - k)\dot{\theta}_2\dot{\theta}_3\theta_2\right\} \\ + I_{33}\ddot{\theta}_3 + H(\theta_1\dot{\theta}_1 + \theta_2\dot{\theta}_2). \quad (18)$$

Equation (16) can be written as

$$T_1 = H\left\{\frac{I_{11}}{H}(\ddot{\theta}_1 - \ddot{\theta}_3\theta_2 - \dot{\theta}_3\dot{\theta}_2) - (\dot{\theta}_2 + \dot{\theta}_3\theta_1)\right\}.$$

By using the values given by NASA for I_{11} and H , we have

$$T_1 = H \left\{ \left(\ddot{\theta}_1 - \ddot{\theta}_3 \theta_2 - \dot{\theta}_3 \dot{\theta}_2 \right) \cdot 10^{-3} - \left(\dot{\theta}_2 + \dot{\theta}_3 \theta_1 \right) \right\} .$$

Therefore, if the magnitudes of I_{11} and I_{22} are much smaller than the magnitude of H , and if θ_1 , θ_2 , and θ_3 , and their derivatives are small, then the equations will be simplified as follows:

$$\begin{aligned} T_1 &= -H \left(\dot{\theta}_2 + \dot{\theta}_3 \theta_1 \right) , \\ T_2 &= H \left(\dot{\theta}_1 - \dot{\theta}_3 \theta_2 \right) , \\ T_3 &= I \ddot{\theta}_3 + H \left(\theta_1 \dot{\theta}_1 + \theta_2 \dot{\theta}_2 \right) , \end{aligned} \tag{19}$$

where $I = I_{11} + I_{22} + I_{33}$. This is a simplified equation for the control element. If the approximation given by Eq. (3) is not acceptable and G_3 must be $\tilde{I}_3 \ddot{\theta}_3$, then I should be equal to $I_{11} + I_{22} + I_{33} + \tilde{I}_3$ in Eq. (19).

The equation of motion of the controlled part (platform) is described as

$$\begin{aligned} I_x \ddot{\theta}_x &= M_x \\ I_y \ddot{\theta}_y &= M_y \\ I_z \ddot{\theta}_z &= M_z , \end{aligned}$$

and using the relationship between M and T yields

$$\begin{aligned}
I_x \ddot{\theta}_x &= T_1 \cos \theta_3 - T_2 \sin \theta_3 \\
I_y \ddot{\theta}_y &= T_2 \cos \theta_3 + T_1 \sin \theta_3 \\
I_z \ddot{\theta}_z &= T_3 \quad .
\end{aligned} \tag{20}$$

The values of I_x , I_y , and I_z are given by NASA as 40,000, 40,000, and 20,000 slug-ft², respectively.

Although Eqs. (19) and (20) still have nonlinear terms, they are much easier to handle than the original one.

Let us introduce the state variables $\underline{x}^T = [x_1, x_2, \dots, x_{10}]$ and the control value $\underline{u}^T = [u_1, u_2, u_3]$ as follows:

$$\begin{aligned}
x_1 &= \theta_x & x_6 &= \dot{\theta}_z & u_1 &= \dot{\theta}_1 \\
x_2 &= \dot{\theta}_x & x_7 &= \theta_1 & u_2 &= \dot{\theta}_2 \\
x_3 &= \theta_y & x_8 &= \theta_2 & u_3 &= \ddot{\theta}_3 \\
x_4 &= \dot{\theta}_y & x_9 &= \theta_3 & & \\
x_5 &= \theta_z & x_{10} &= \dot{\theta}_3 & &
\end{aligned} \quad .$$

Using these new variables, we can write Eqs. (19) and (20) as

$$\begin{aligned}
T_1 &= -H(u_2 + x_7 x_{10}) \\
T_2 &= H(u_1 - x_8 x_{10}) \\
T_3 &= I u_3 + H(x_8 u_2 + x_7 u_1)
\end{aligned} \tag{21}$$

$$\begin{aligned}
\dot{x}_1 &= x_2 \\
\dot{x}_2 &= \frac{1}{I_x} \left[T_1 \cos x_9 - T_2 \sin x_9 \right] \\
\dot{x}_3 &= x_4 \\
\dot{x}_4 &= \frac{1}{I_y} \left[T_2 \cos x_9 + T_1 \sin x_9 \right] \\
\dot{x}_5 &= x_6 \\
\dot{x}_6 &= \frac{1}{I_z} T_3 \\
\dot{x}_7 &= u_1 \\
\dot{x}_8 &= u_2 \\
\dot{x}_9 &= x_{10} \\
\dot{x}_{10} &= u_3
\end{aligned} \tag{22}$$

Substituting Eq. (21) for Eq. (22) results in the following:

$$\begin{aligned}
\dot{x}_1 &= x_2 \\
\dot{x}_2 &= -\frac{H}{I_x} \left[x_7 x_{10} \cos x_9 - x_8 x_{10} \sin x_9 \right] - \left(\frac{H}{I_x} \sin x_9 \right) u_1 - \left(\frac{H}{I_x} \cos x_9 \right) u_2 \\
\dot{x}_3 &= x_4 \\
\dot{x}_4 &= -\frac{H}{I_y} \left[x_8 x_{10} \cos x_9 + x_7 x_{10} \sin x_9 \right] + \left(\frac{H}{I_y} \cos x_9 \right) u_1 - \left(\frac{H}{I_y} \sin x_9 \right) u_2 \\
\dot{x}_5 &= x_6 \\
\dot{x}_6 &= \frac{H}{I_z} x_7 u_1 + \frac{H}{I_z} x_8 u_2 + \frac{I}{I_z} u_3 \\
\dot{x}_7 &= u_1 \\
\dot{x}_8 &= u_2 \\
\dot{x}_9 &= x_{10} \\
\dot{x}_{10} &= u_3
\end{aligned} \tag{23}$$

C. Cost Function

The next subject of discussion is the cost function, which is the sum of the power consumption and time, with a weighting parameter; it is expressed as

$$J = \int_{t_0}^{t_1} \left\{ |T_1 \dot{\theta}_1| + |T_2 \dot{\theta}_2| + |T_3 \dot{\theta}_3| + k \right\} dt \quad . \quad (24)$$

Although T_1 , T_2 , and T_3 satisfy Eqs. (19) after some approximations, we will approximate them further as follows:

$$T_1 = -H\dot{\theta}_2$$

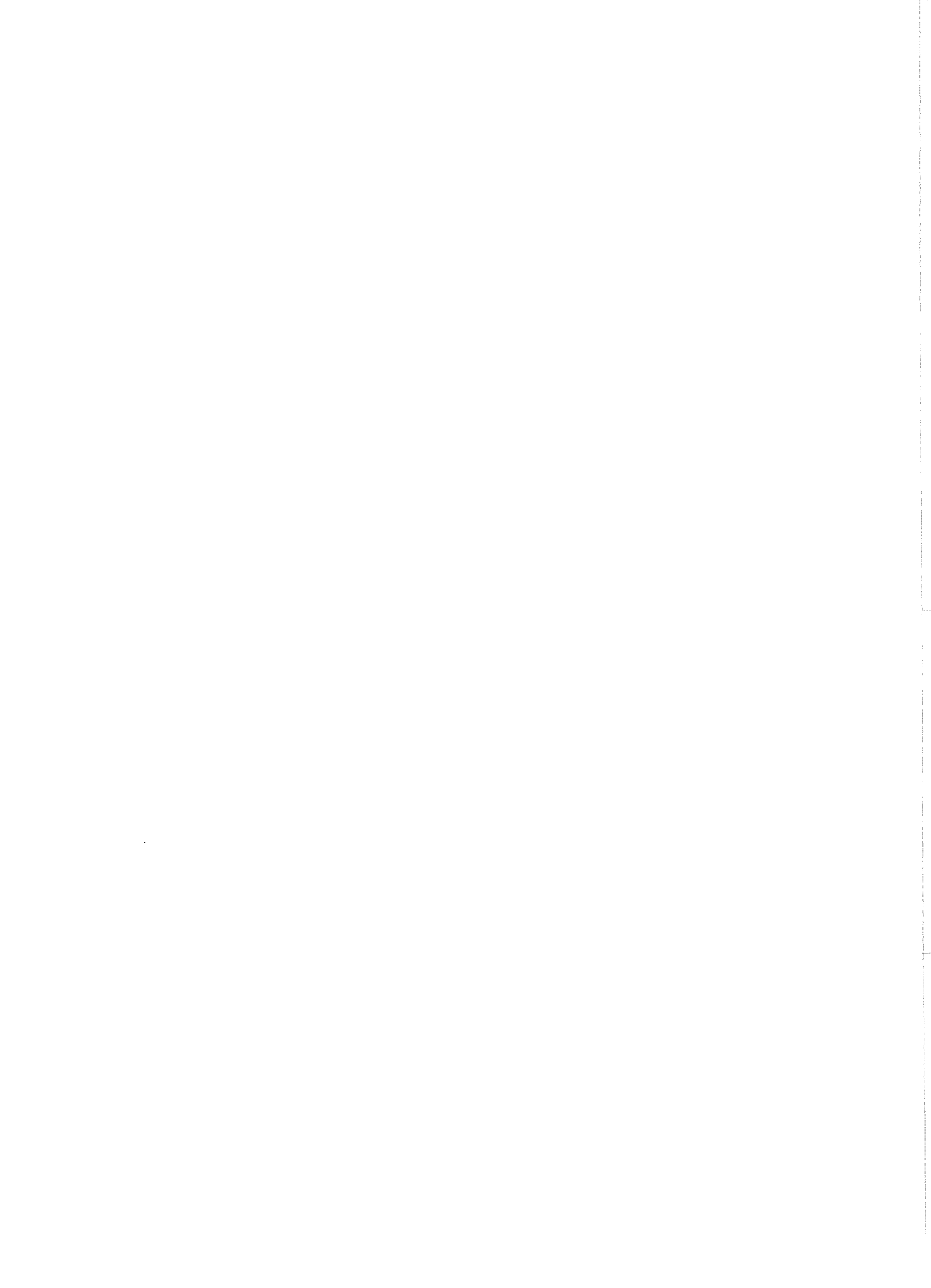
$$T_2 = H\dot{\theta}_1$$

$$T_3 = -I_3\ddot{\theta}_3 \quad .$$

Then the cost function described by Eq. (24) will become

$$J = \int_{t_0}^{t_1} \left[2 |H u_1 u_2| + |I x_{10} u_3| + k \right] dt \quad . \quad (25)$$

The approximation above is well justified for small values of θ_1 , θ_2 , θ_3 , and their derivatives.



IV OPTIMIZATION

A. Simplification

One of the objectives of this research is to find the optimum control laws for u_1 , u_2 , and u_3 that will drive disturbances to the stationary position in minimum time. During the course of this research (as described in Section IV-C), it was found that the outer gimbal cannot successfully be used as a torque generator. The outer gimbal is simply used for eliminating the z-axis torque produced by the inner and middle gimbal movements while controlling the θ_x , θ_y disturbances. In other words, u_3 is chosen so as to make \dot{x}_6 zero. From Eqs. (23), u_3 can be expressed as

$$u_3 = -\frac{H}{I} (x_7 u_1 + x_8 u_2) \quad . \quad (26)$$

With this choice of u_3 , the optimum control laws for u_1 and u_2 are derived. Let

$$\begin{aligned} \epsilon_1 &= x_{10} \left[x_7 \cos x_9 - x_8 \sin x_9 \right] \frac{H}{I_x} \quad , \\ \epsilon_2 &= x_{10} \left[x_8 \cos x_9 + x_7 \sin x_9 \right] \frac{H}{I_y} \quad , \\ W_1 &= \left[u_1 \sin x_9 + u_2 \cos x_9 \right] \frac{H}{I_x} \quad , \\ W_2 &= \left[-u_1 \cos x_9 + u_2 \sin x_9 \right] \frac{H}{I_y} \quad . \end{aligned} \quad (27)$$

Then Eqs. (23) will become,

$$\begin{aligned}
\dot{x}_1 &= x_2 \\
\dot{x}_2 &= -\left[\epsilon_1 + W_1\right] \\
\dot{x}_3 &= x_4 \\
\dot{x}_4 &= -\left[\epsilon_2 + W_2\right]
\end{aligned}
\tag{28}$$

Before further analysis, let us review the maximum principle of Pontryagin.

B. Application of Maximum Principle

Let us consider the time-optimal control of the system described by Eqs. (28). If there is no bound for u_1 and u_2 , there is no solution. Hence u_1 and u_2 are considered to be bounded and are described as

$$\begin{aligned}
|u_1| &\leq \alpha \quad , \\
|u_2| &\leq \alpha \quad .
\end{aligned}
\tag{29}$$

The optimal control problem is defined as follows: The system is described by Eqs. (28) and (29). The objective is to determine control laws $u_1(t)$ and $u_2(t)$, which drive x_1 , x_2 , x_3 , and x_4 to zero at the final time and which minimize the function

$$J_1 = \int_{t_0}^{t_1} 1 \, dt
\tag{30}$$

along the solution.

Introducing the four-dimensional adjoint vector $\underline{\lambda}^T = (\lambda_1, \lambda_2, \lambda_3, \lambda_4)$ and the function

$$\mathfrak{H}(\underline{\lambda}, \underline{x}, \underline{u}) = \sum_{i=1}^4 \lambda_i \dot{x}_i \quad , \quad (31)$$

we have the equations

$$\dot{x}_i = \frac{\partial \mathfrak{H}}{\partial \lambda_i} \quad , \quad (32)$$

$$\dot{\lambda}_i = - \frac{\partial \mathfrak{H}}{\partial x_i} \quad . \quad (33)$$

For fixed values of $\underline{\lambda}$ and \underline{x} , \mathfrak{H} is a function of \underline{u} . We denote the upper bound of the values of this function by $M(\underline{\lambda}, \underline{x})$:

$$M(\underline{\lambda}, \underline{x}) = \text{Sup}_{u \in U} \mathfrak{H}(\underline{\lambda}, \underline{x}, \underline{u}) \quad . \quad (34)$$

Maximum Principle³--Let $\underline{u}(t)$, $t_0 \leq t \leq t_1$ be an admissible control that transfers the state point from \underline{x}_0 to \underline{x}_1 , and let $\underline{x}(t)$ be the corresponding trajectory, so that $\underline{x}(t_0) = \underline{x}_0$, $\underline{x}(t_1) = \underline{x}_1$. In order that $\underline{u}(t)$ and \underline{x} be time-optimal, it is necessary that there exist a nonzero, continuous vector function $\underline{\lambda}^T(t) = [\lambda_1(t), \lambda_2(t), \lambda_3(t), \lambda_4(t)]$ corresponding to $\underline{u}^*(t)$ and $\underline{x}^*(t)$ such that

- (1) For all t , $t_0 \leq t \leq t_1$, the function $\mathfrak{H}[\underline{\lambda}(t), \underline{x}(t), \underline{u}]$ of the variable $u \in U$ attains its maximum at the point $\underline{u} = \underline{u}^*(t)$:

$$\mathfrak{H}[\underline{\lambda}(t), \underline{x}^*(t), \underline{u}^*(t)] = M(\underline{\lambda}, \underline{x}) \quad , \quad (35)$$

- (2) At the terminal time t_1 , the relation

$$M[\underline{\lambda}(t_1), \underline{x}(t_1)] \geq 0 \quad (36)$$

is satisfied.

Furthermore, it turns out that if $\underline{\lambda}(t)$, $\underline{x}(t)$, and $\underline{u}(t)$ satisfy system (32), (33), and condition (1), the time function $M[\underline{\lambda}(t), \underline{x}(t)]$ is constant. Thus Eq. (36) may be verified at any time t , $t_0 \leq t \leq t_1$, and not just at t_1 .

C. Minimum Time Control

Let us apply the maximum principle to the problem described by relations (28), (29), and (30). Variables ϵ_1 and ϵ_2 are considered to be constant during the process of finding an optimal control law. Once the optimal control is found, ϵ_1 and ϵ_2 are considered to be variables as defined by Eqs. (27). This type of approach is used frequently. The representative example is the Kryloff-Bogoliuboff method in nonlinear mechanics.⁴

If ϵ_1 and ϵ_2 are treated as constants, then Eqs. (28) are decoupled. The optimal control laws for W_1 are obtained by using the maximum principle of Pontryagin as follows.

The Hamiltonian function \mathcal{H} for a set of equations

$$\begin{aligned}\dot{x}_1 &= x_2 \\ \dot{x}_2 &= -\left[\epsilon_1 + W_1\right]\end{aligned}$$

is described as

$$\mathcal{H} = \lambda_1 x_2 - \lambda_2 (\epsilon_1 + W_1) \quad .$$

The adjoint variables λ_1 and λ_2 satisfy the differential equations

$$\dot{\lambda}_1 = -\frac{\partial H}{\partial x_1} = 0 \quad ,$$

$$\dot{\lambda}_2 = -\frac{\partial H}{\partial x_2} = -\lambda_1 \quad .$$

Hence the optimum control law for W_1 becomes

$$W_1^* = \alpha \frac{H}{I_x} \operatorname{sgn}(-\lambda_2) = \bar{\alpha} \operatorname{sgn}(-\lambda_2) \quad (37)$$

and W_1^* has at most one switch. The construction of a switching curve in the x_1 - x_2 plane is done by analyzing the backward trajectories starting from the origin.

Let $\tau = t_f - t$ and $d/dt = ()'$; then we have

$$x_1' = -x_2$$

$$x_2' = \epsilon_1 + W_1 \quad ,$$

where T is constant. If $W_1 = \pm \bar{\alpha}$, then x_2 and x_1 are given by

$$x_2 = (\epsilon_1 \pm \bar{\alpha})\tau$$

$$x_1 = -\frac{\epsilon_1 \pm \bar{\alpha}}{2} \tau^2 = \frac{x_2^2}{2(\bar{\alpha} \mp \epsilon_1)} \quad .$$

Hence, we have

$$W_1^* = \bar{\alpha} \operatorname{sgn} \left[x_1 + \frac{x_2 |x_2|}{2\bar{\alpha} - \epsilon_1 \operatorname{sgn} x_1} \right] \quad . \quad (38)$$

Similarly,

$$W_2^* = \bar{\alpha} \operatorname{sgn} \left[x_3 + \frac{x_4 |x_4|}{2\bar{\alpha} - \epsilon_2 \operatorname{sgn} x_3} \right] . \quad (39)$$

By substituting W_1^* and W_2^* into Eqs. (27), we find the optimal control laws u_1^* and u_2^* to be

$$u_1^* = \alpha \sin x_9 \cdot \operatorname{sgn} \left[x_1 + \frac{x_2 |x_2|}{2\bar{\alpha} - \epsilon_1 \operatorname{sgn} x_1} \right] - \alpha \cos x_9 \cdot \operatorname{sgn} \left[x_3 + \frac{x_4 |x_4|}{2\bar{\alpha} - \epsilon_2 \operatorname{sgn} x_3} \right] , \quad (40)$$

$$u_2^* = \alpha \sin x_9 \cdot \operatorname{sgn} \left[x_3 + \frac{x_4 |x_4|}{2\bar{\alpha} - \epsilon_2 \operatorname{sgn} x_3} \right] + \alpha \cos x_9 \cdot \operatorname{sgn} \left[x_1 + \frac{x_2 |x_2|}{2\bar{\alpha} - \epsilon_1 \operatorname{sgn} x_1} \right] . \quad (41)$$

It should be noted that these optimal control laws are not designed for driving gimbal angles to zero when the disturbances of the space vehicle are controlled to the desired position.

At the early part of this section, it is mentioned that the outer gimbal is not a good torque generator. Let us examine this fact further.

The optimal control law for the outer gimbal is not successfully obtained. This is due to the fact that the torque produced by rotating the outer gimbal is not sufficiently large to control the disturbances about the z axis. The present device can control the disturbances about the z axis but it takes an unreasonable length of time. One way to make the present system workable is to increase the moment of inertia of the outer gimbal. This may not be acceptable for many reasons. The restrictions on physical sizes and weights are two of these reasons. It is

hence necessary to add an additional torque generator in order to control the z-axis disturbances properly. It should be pointed out that the present outer gimbal has its own function, which is expressed in Eqs. (23) and (26). Assume $u_1 = u_2 = 0$ in Eqs. (23); then x_5 and x_6 should satisfy the differential equations

$$\begin{aligned}\dot{x}_5 &= x_6 \quad , \\ \dot{x}_6 &= \frac{I}{I_z} u_3 \quad , \quad |u_3| \leq \beta \quad .\end{aligned}$$

Hence the minimum time control law for u_3 is described as

$$u_3 = -\beta \operatorname{sgn} \left[x_5 + \frac{I}{2I\beta} x_6 |x_6| \right] \quad .$$

After a tedious calculation, it can be shown that the time t_f required for driving the initial state $(x_5, x_6) = (a, b)$ to the origin is expressed as

$$t_f = \frac{b + \sqrt{2(b^2 + 2a\delta)}}{\delta} \quad ,$$

where $\delta = I\beta/I_z$ and $a + b|b|/2\delta > 0$.

For the present system, $I = 13 \text{ slug-ft}^2$, $I_z = 20,000 \text{ slug-ft}^2$, and $\beta = 0.1745 \text{ rad/s}^2$. Hence

$$\delta = \frac{I\beta}{I_z} = 1.134 \times 10^{-4} \quad \text{rad/s}^2 \quad .$$

If the initial values are chosen to be $a = 0$ and $b = 1.2 \times 10^{-3} \text{ rad/s}$, then

$$t_f = \frac{(1 + \sqrt{2}) b}{\delta} = 25.5 \quad \text{seconds} \quad .$$

This clearly shows that the outer gimbal cannot control the high-frequency disturbances about the z axis. One way to improve this is to increase the value of δ by increasing I and/or β . This point needs further investigation.

D. Examples of Minimum Time Control

The optimal control laws u_1^* and u_2^* are tested by applying them to different types of disturbances. Since θ_x and θ_y behave similarly to the same type of disturbances, only the disturbances for θ_x are considered.

If the forcing term about the x axis is described as \bar{M}_x , then θ_x satisfies the differential equation

$$I \ddot{\theta}_x = \bar{M}_x \quad .$$

For our tests, \bar{M}_x is chosen to be step input, ramp input, and sinusoidal inputs with different frequencies. Figures 2(a) and 2(b) show the behavior of θ_x under the 25 ft-lb input and 5t ft-lb ramp input, respectively. For the examples considered here, the limits of the gimbal rates are expressed as

$$|\dot{\theta}_1| \leq 5^\circ/\text{s} \quad ,$$

$$|\dot{\theta}_2| \leq 5^\circ/\text{s} \quad ,$$

$$|\dot{\theta}_3| \leq 20^\circ/\text{s} \quad .$$

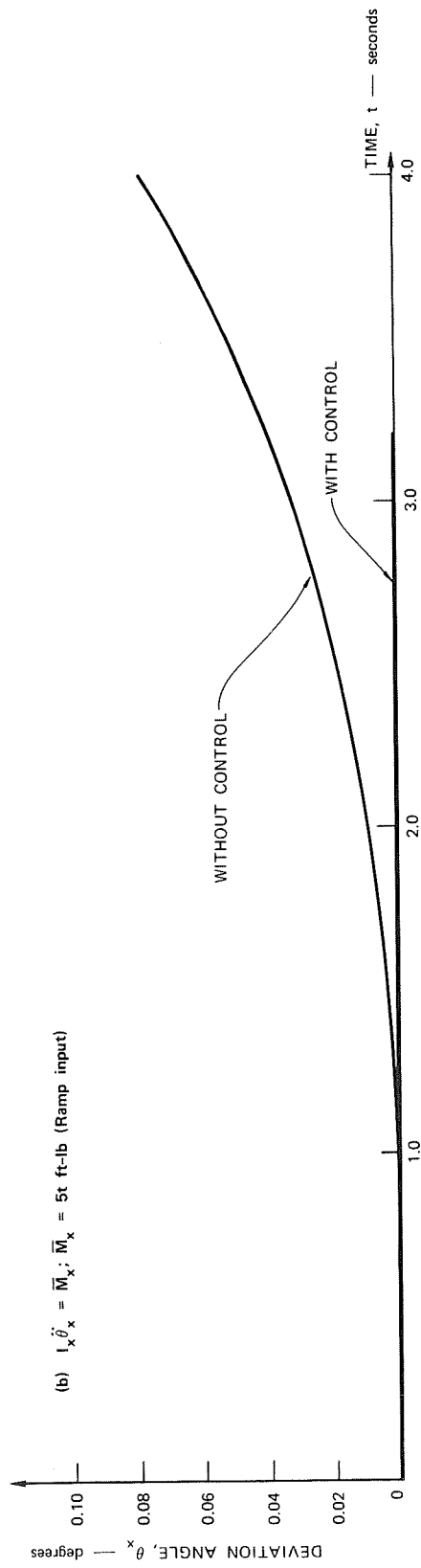
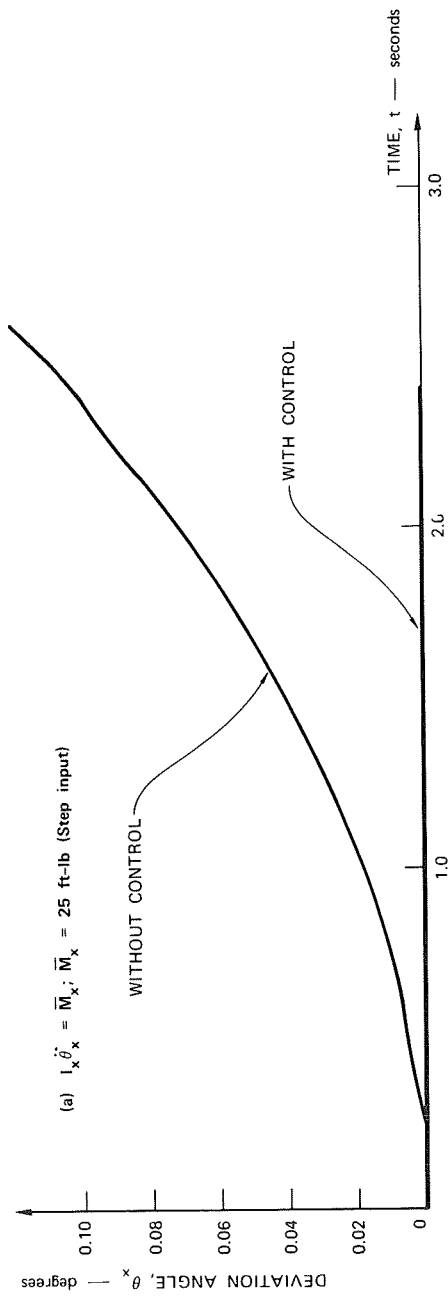


FIGURE 2 BEHAVIOR OF θ_x

TB-7204-2

These conditions determine α to be $\pi/36 = 0.0872$ rad/s; hence this will restrict the motion. The performance is satisfactory. The optimal controller performed well against sinusoidal disturbances also. The sine waves with 10 ft-lb amplitude and 0.5, 2, and 5 c/s are used as disturbances. The results are shown in Figures 3, 4, and 5. Even if the disturbance is only in θ_x , the torque for controlling θ_x disturbs θ_y due to the coupling effect. The maximum deviations of θ_y due to the coupling effect are summarized in Table I.

Table I

MAXIMUM DEVIATION OF θ_y

| Case | Maximum Deviation of θ_y (degrees) |
|---|--|
| Step Input $\bar{M}_x = 25$ ft-lb | 1.0×10^{-5} |
| Ramp Input $\bar{M}_x = 5t$ ft-lb | 1.0×10^{-5} |
| Sinusoidal Input $\bar{M}_x = 10 \sin(\pi t)$ ft-lb | 1.6×10^{-5} |
| $\bar{M}_x = 10 \sin(4\pi t)$ ft-lb | 1.09×10^{-5} |
| $\bar{M}_x = 10 \sin(10\pi t)$ ft-lb | 1.08×10^{-5} |

The optimal control laws are also tested for driving the arbitrary initial states to the origin. The results are shown in Figures 6 and 7.

The optimal laws u_1^* and u_2^* described by Eqs. (40) and (41) are substituted for u_1 and u_2 in Eqs. (23).

If the order of the magnitudes of $\theta_1, \theta_2, \theta_3$, and their derivatives are at most several degrees and several degrees/second, then Eqs. (23) are an acceptable mathematical model for the CMG. The maximum disturbances for θ_x and θ_y (x_1 and x_2) are considered to be less than 0.00075 rad (=0.043 deg). In the case of astronomical observations, disturbances of this magnitude will be expected.

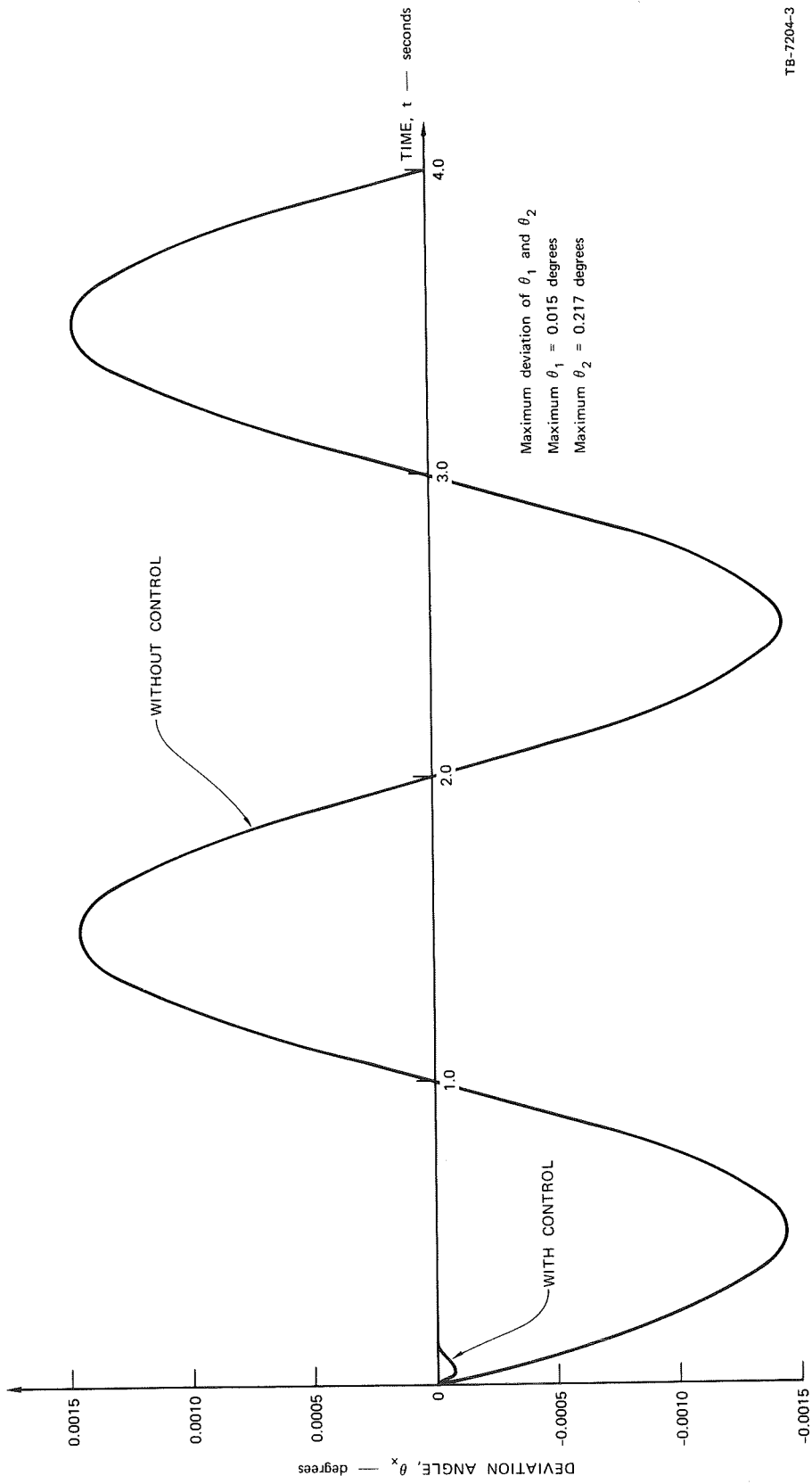
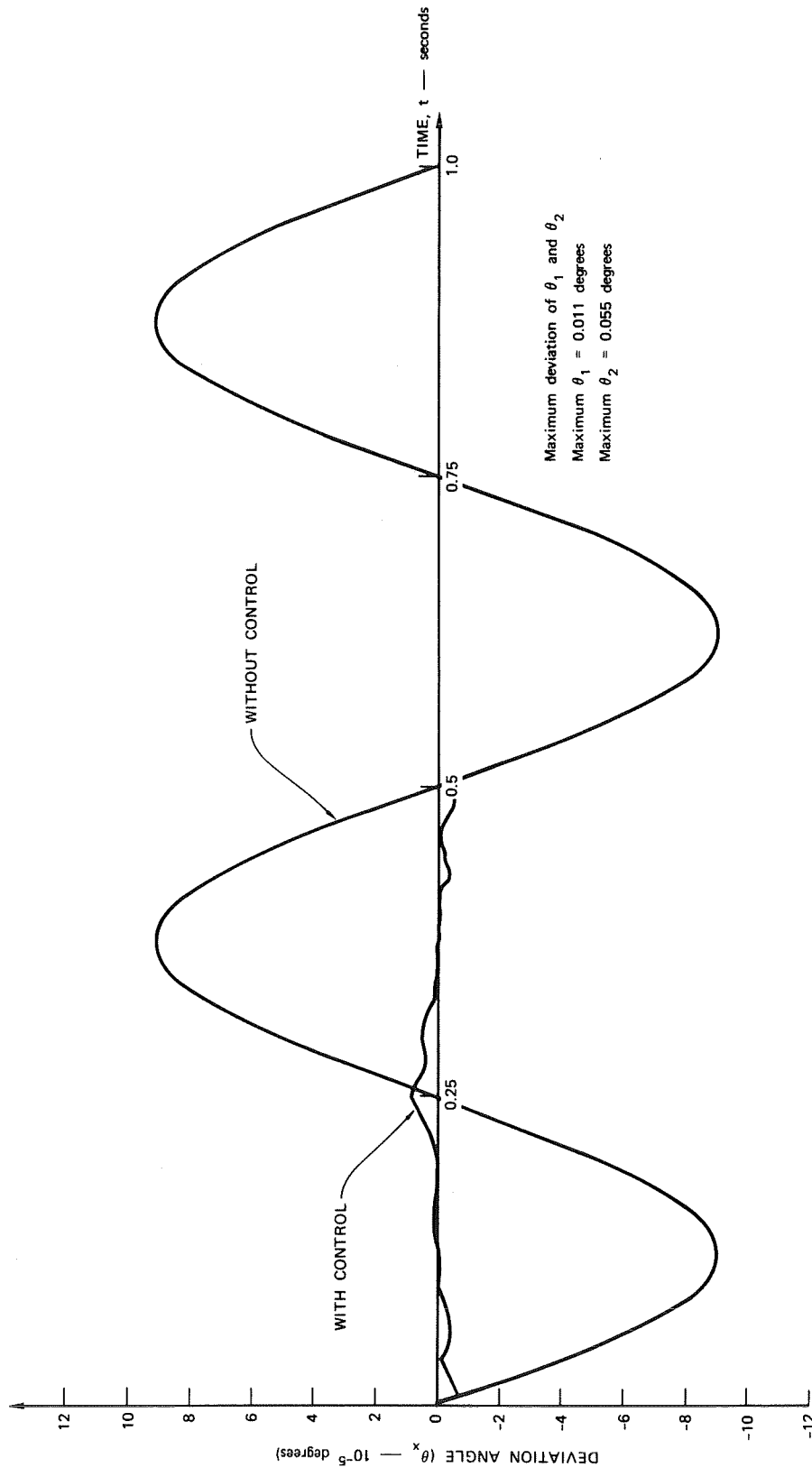


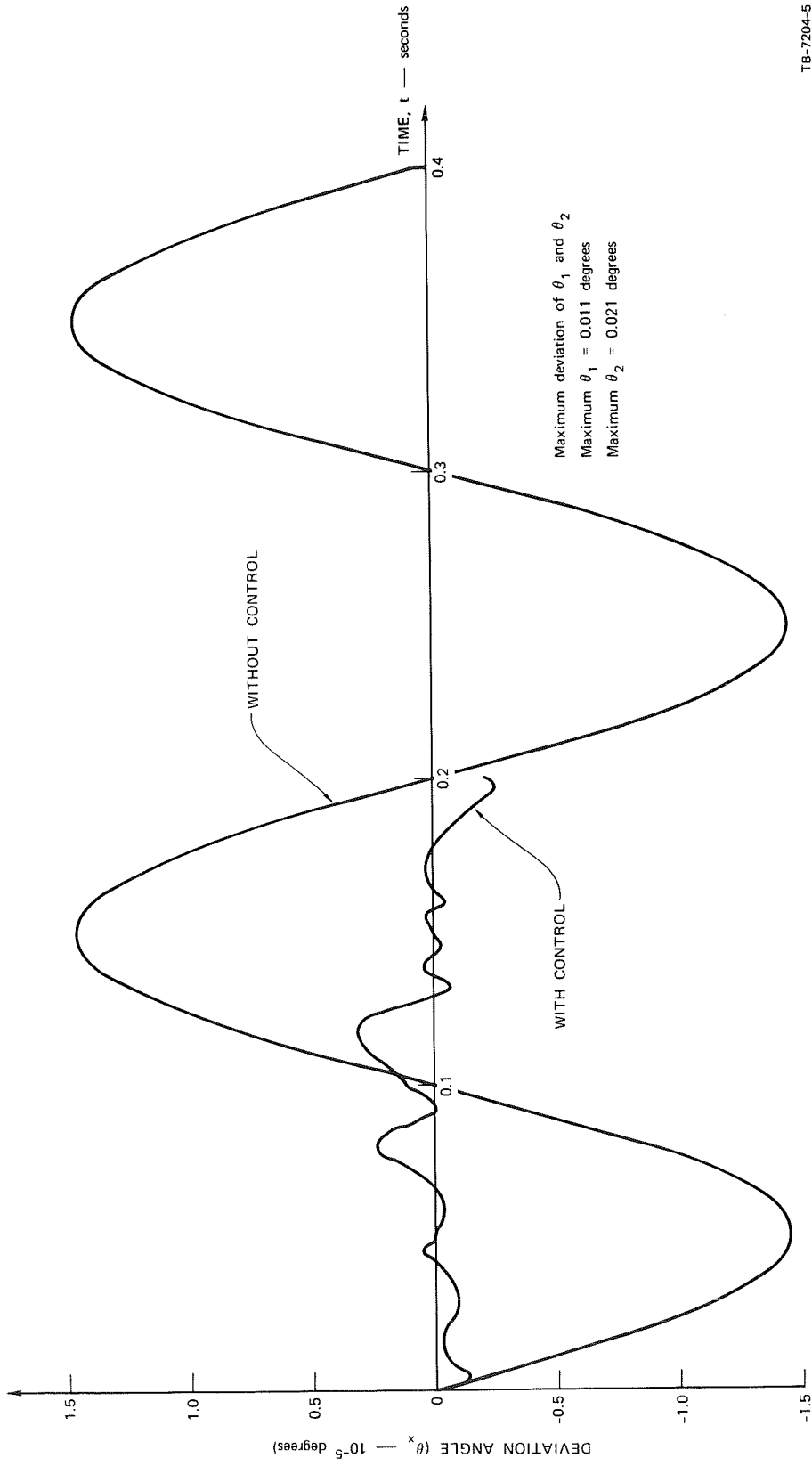
FIGURE 3 $I_x \ddot{\theta}_x = \bar{M}_x; \bar{M}_x = 10 \sin(\pi t)$ ft-lb (0.5 c/s)

TB-7204-3



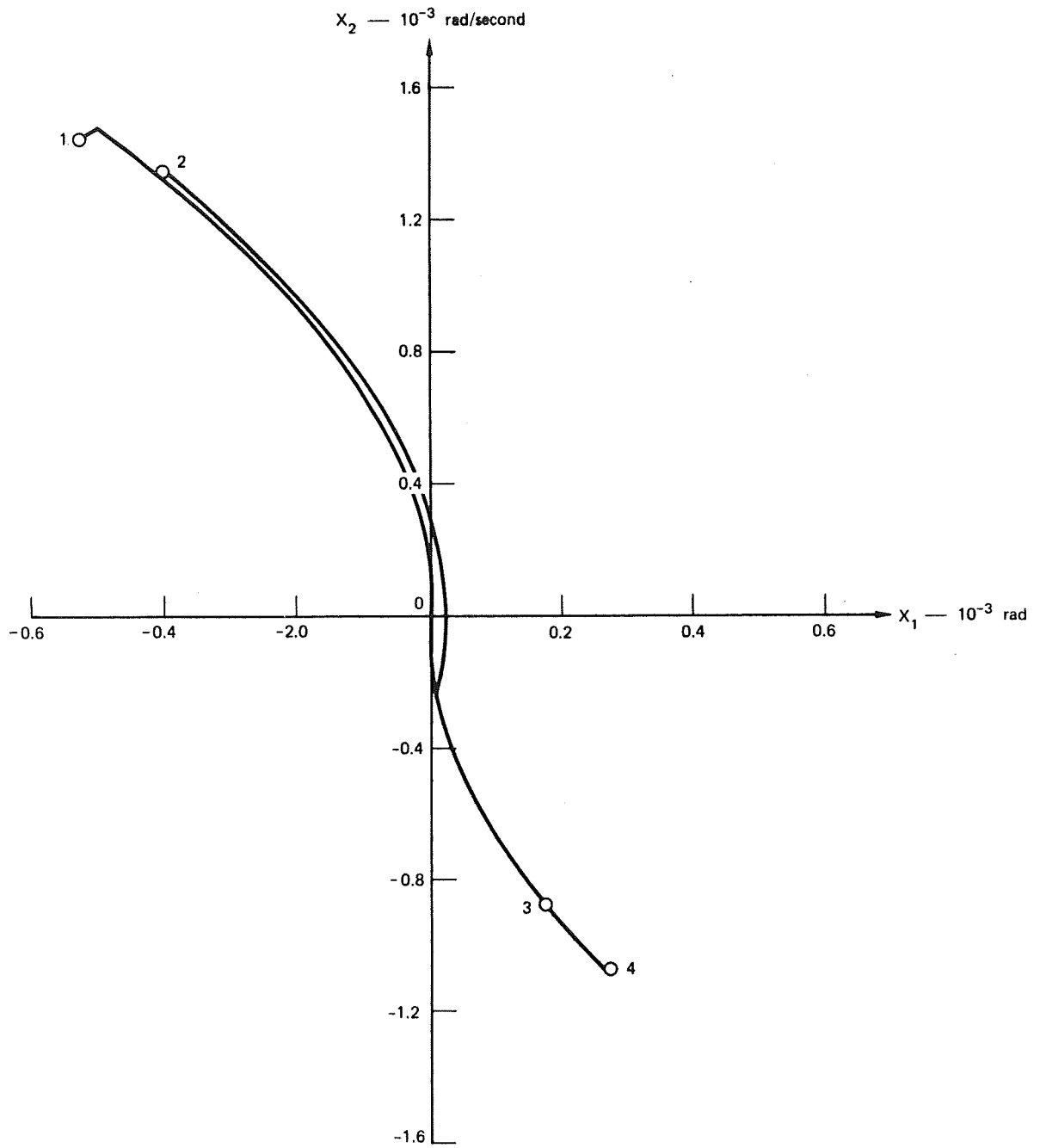
TB-7204-4

FIGURE 4 $I_x \ddot{\theta}_x = \bar{M}_x; \bar{M}_x = 10 \sin(4\pi t)$ ft-lb (2 c/s)



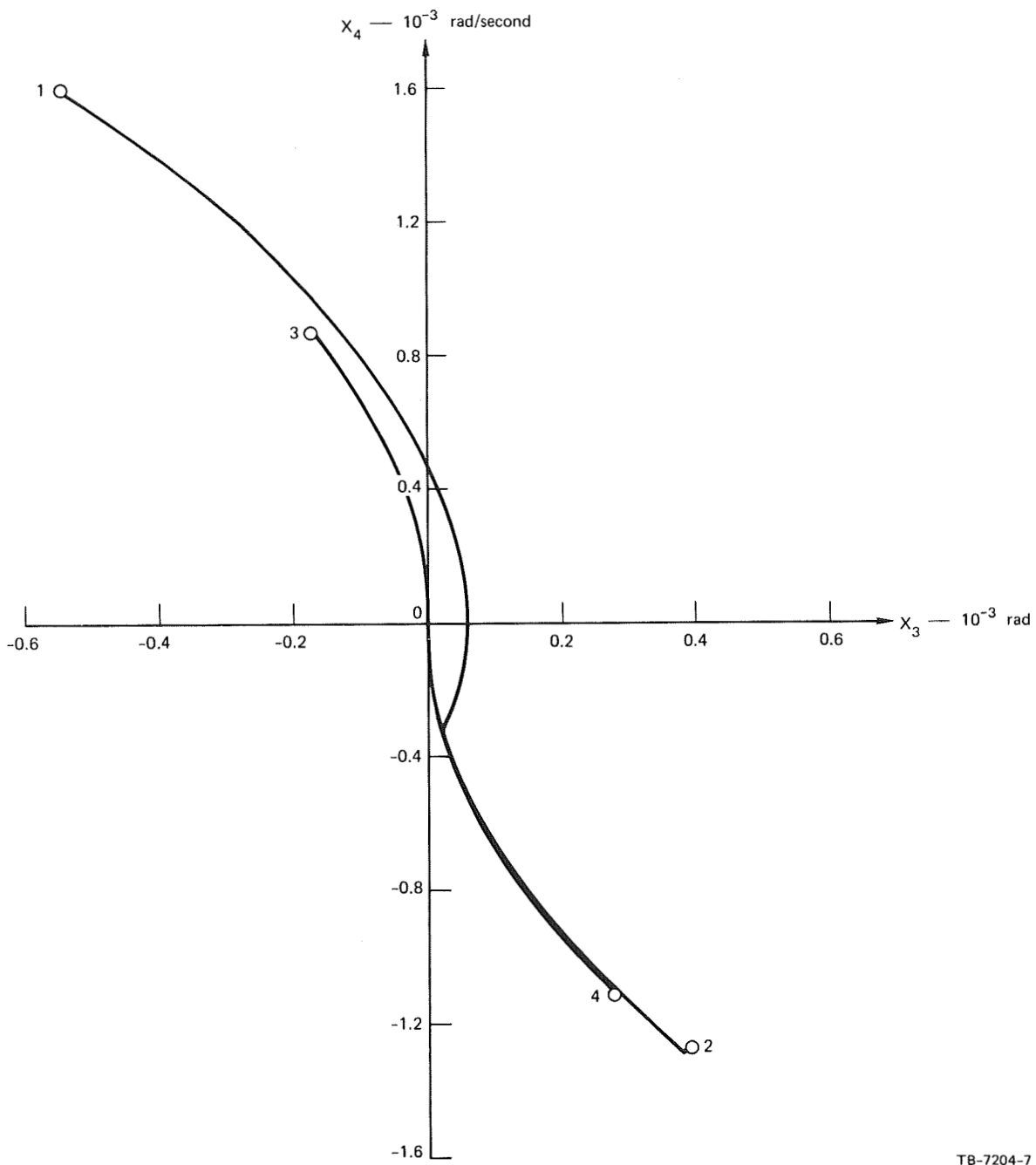
TB-7204-5

FIGURE 5 $I_x \ddot{\theta}_x = \bar{M}_x; \bar{M}_x = 10 \sin(10\pi t)$ ft-lb (5 c/s)



TB-7204-6

FIGURE 6 SUBOPTIMAL TRAJECTORIES ($x_1 - x_2$ plane)



TB-7204-7

FIGURE 7 SUBOPTIMAL TRAJECTORIES ($x_3 - x_4$ plane)

The theoretical optimum time is known for each initial state numbered 1 to 4. The time required to reach the circular region with radius of 10^{-5} radian about the origin of the x_1-x_3 plane is calculated for each initial state and shown in Table II.

Table II

COMPARISON OF TIME REQUIREMENT

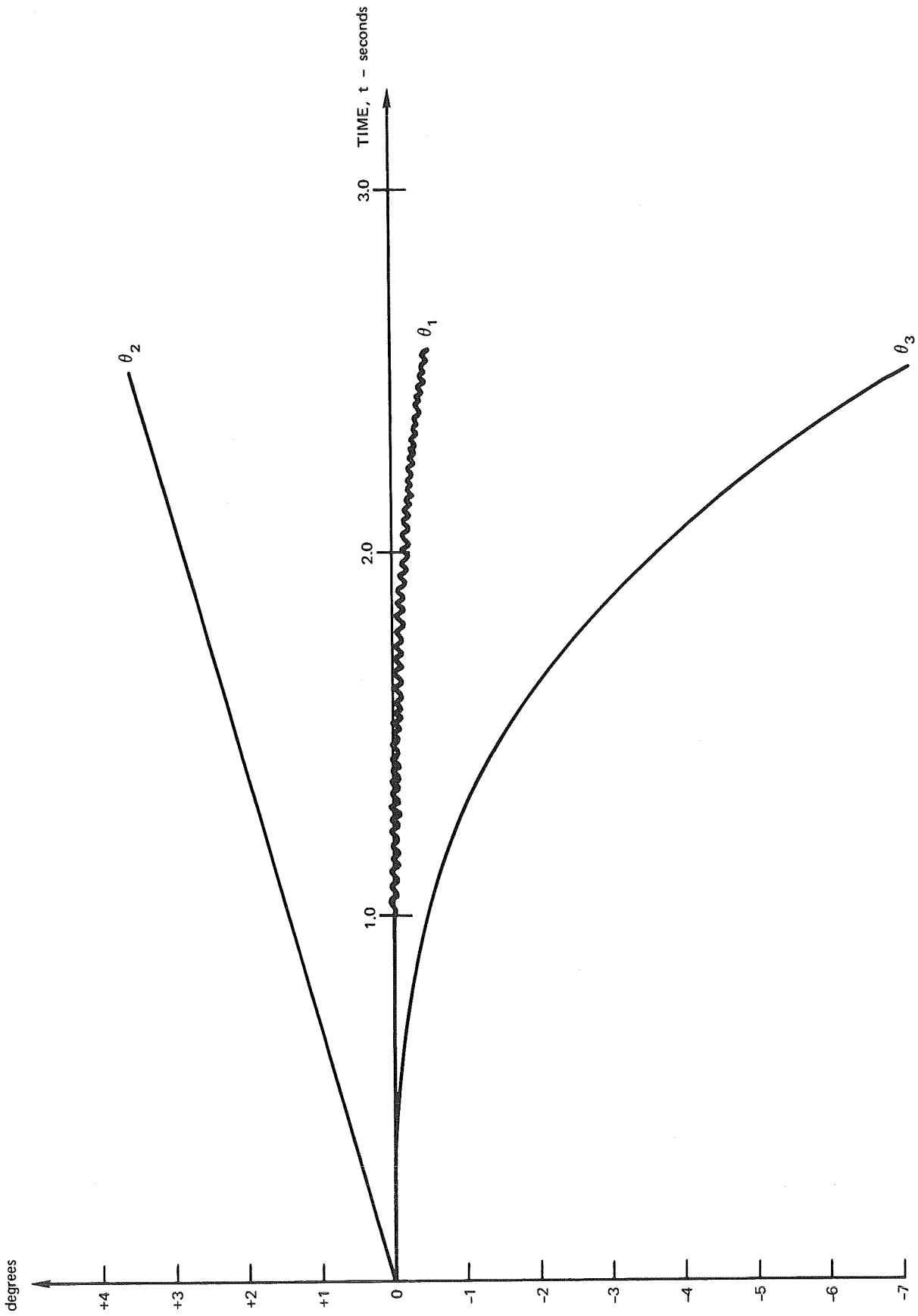
| Initial State | Theoretical Optimum Time (seconds) | Time Required to Reach the Region with Radius of 10^{-5} rad in x_1-x_3 Plane (seconds) |
|---------------|------------------------------------|---|
| 1 | 0.702 | 1.023 |
| 2 | 0.602 | 0.772 |
| 3 | 0.402 | 0.420 |
| 4 | 0.502 | 0.535 |

The behavior of the gimbals during these controls is a valuable piece of information. The time histories of the motion of CMG gimbals for step input, sinusoidal input (0.5 c/s) and the arbitrary initial disturbances that correspond to initial states 2 and 3 in Figures 6 and 7 are shown in Figures 8, 9, and 10.

In conclusion, the tests proved that the optimal control laws u_1^* and u_2^* are acceptable for small disturbances.

E. Minimum Power Control

In this section, the minimum power control problem is considered. Because of the same reason mentioned in the minimum time control problem, the outer gimbal is not used for controlling the z-axis disturbances. We will only consider the disturbances about the x and y axes.



TA-7204-8

FIGURE 8 BEHAVIOR OF GIMBALS; $\bar{M}_X = 25$ ft-lb. (Step input.)

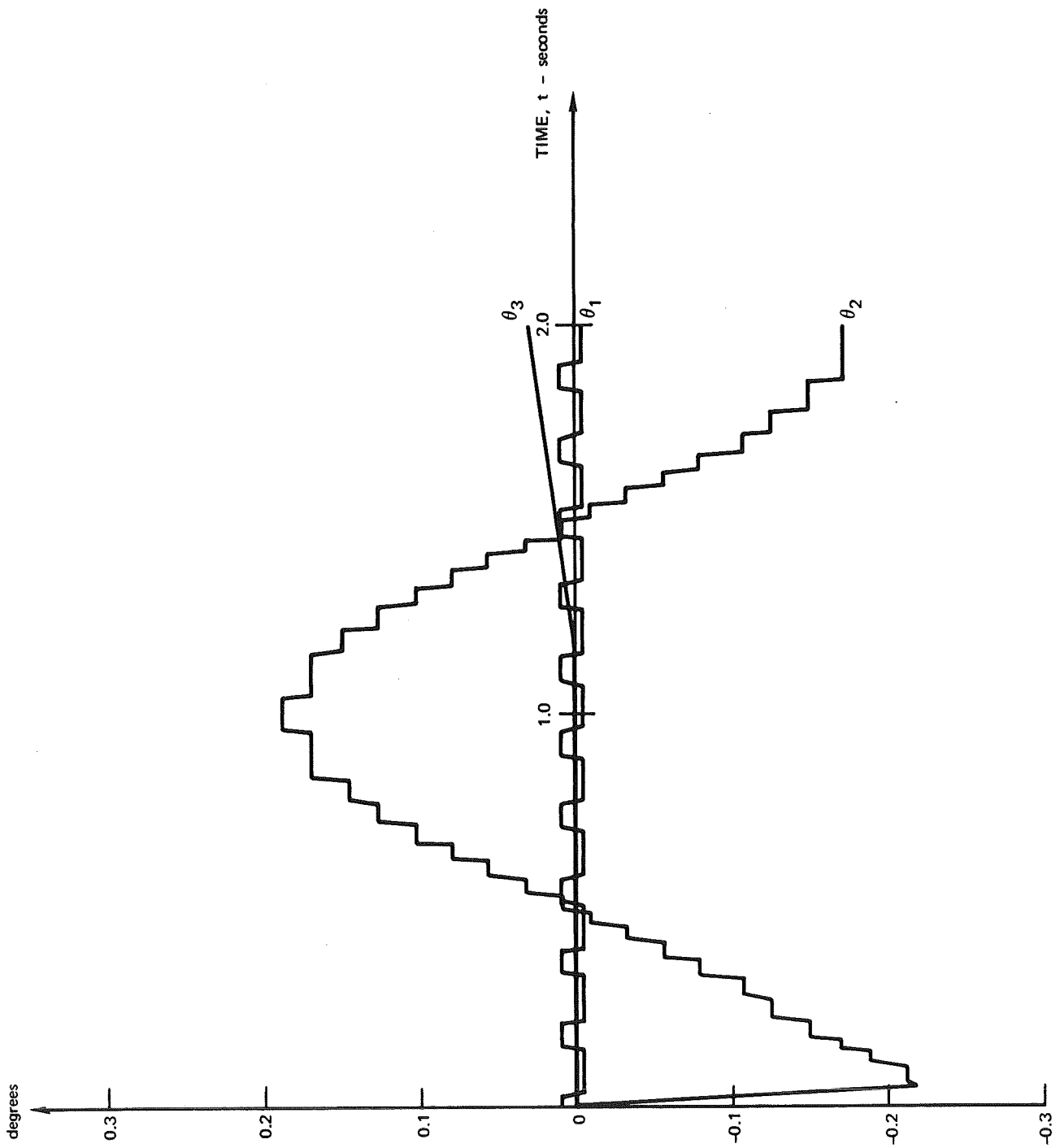
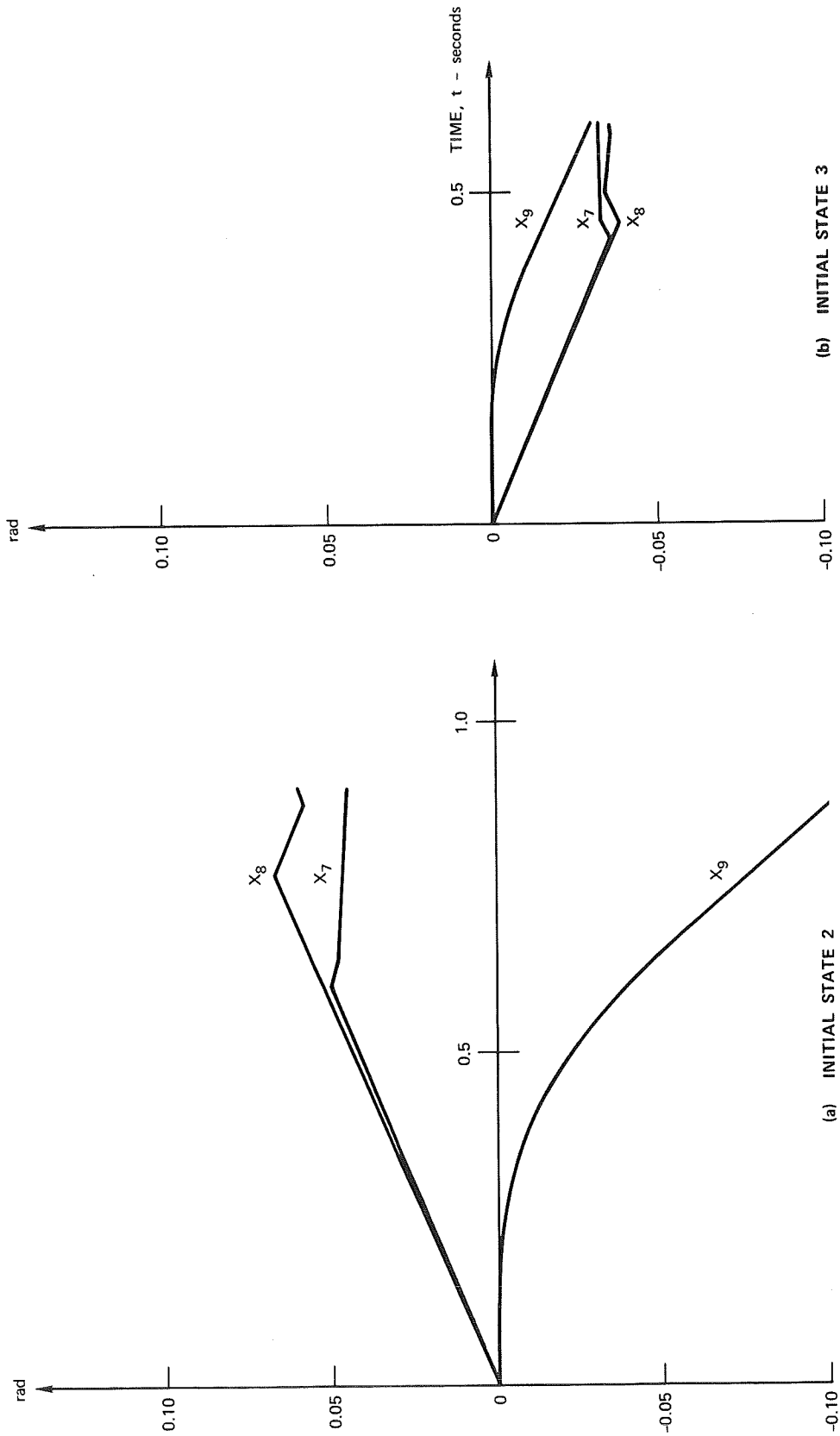


FIGURE 9 BEHAVIOR OF GIMBALS; $\bar{M}_x = 10 \sin(\pi t)$ ft-lb (0.5 c/s)



TB-7204-10

FIGURE 10 BEHAVIOR OF GIMBALS

By using the same notations ϵ_1 , ϵ_2 , W_1 , and W_2 defined in Eqs. (27), Eqs. (23) become

$$\dot{x}_1 = x_2$$

$$\dot{x}_2 = -[\epsilon_1 + W_1]$$

$$\dot{x}_3 = x_4$$

$$\dot{x}_4 = -[\epsilon_2 + W_2] \quad ,$$

which are exactly the same as Eqs. (28).

A cost function for the minimum power problem is expressed as

$$J_2 = \int_0^{t_1} [2\bar{k}|H u_1 u_2| + \bar{k}|I x_{10} u_3| + 1] dt \quad ,$$

where \bar{k} is a weighting factor. If $\bar{k} = 0$, the problem is reduced to the minimum time problem; if $\bar{k} = +\infty$, the problem becomes a pure minimum power problem. The minimum time problem was discussed in the preceding section. A pure minimum power problem is not of interest here because the solution is the one that requires an infinite time to control any disturbance.

The problem considered here is then to minimize both the energy consumption and the time with a certain weighting factor.

If $J_3 = \int_0^t [2\bar{k}|H u_1 u_2| + 1] dt$ is acceptable as an approximation of J_2 , then the optimal control laws for this problem are found in the following way. By treating ϵ_1 and ϵ_2 as constants, we can decouple the differential equations and find the optimal control laws \bar{u}_1 and \bar{u}_2 for u_1 and u_2 independently.

The optimal control law \bar{u}_1 should transfer the initial state to the origin by satisfying the relationships

$$\begin{aligned} \dot{x}_1 &= x_2 \quad , \\ \dot{x}_2 &= -\left[\epsilon_1 + W_1\right] \quad , \\ W_1 &= \left[u_1 \sin x_9 + u_2 \cos x_9\right] \frac{H}{I_x} \quad , \\ |u_1| &\leq \alpha \end{aligned} \tag{42}$$

and by minimizing the cost function

$$J_3 = \int_{t_0}^{t_1} \left[2\bar{k}|H u_1 u_2| + 1\right] dt \quad . \tag{43}$$

The Hamiltonian function for this problem is

$$\mathfrak{H} = \lambda_1 x_2 - \lambda_2 \left[\epsilon_1 + W_1\right] - 2\bar{k}|H u_1 u_2| - 1 \quad . \tag{44}$$

If $u_2 = \pm\alpha(\alpha > 0)$, then W_1 is given by

$$W_1 = \left[u_1 \sin x_9 \pm \alpha \cos x_9\right] \frac{H}{I_x} \quad ,$$

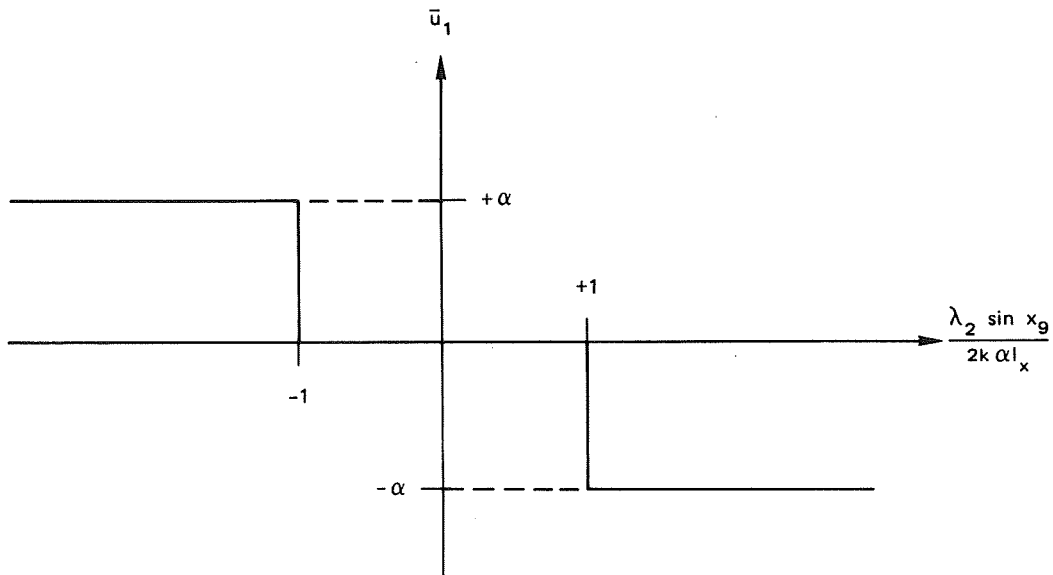
and hence

$$\mathfrak{H} = \lambda_1 x_2 - \lambda_2 \epsilon_1 \mp \lambda_2 \alpha \frac{H}{I_x} \cos x_9 - 2\bar{k}\alpha H \left[\frac{\lambda_2 \sin x_9}{2\bar{k}\alpha I_x} u_1 + |u_1| \right] - 1 \quad .$$

Therefore the optimum \bar{u}_1 that maximizes H is described as

$$\bar{u}_1 = -\alpha \operatorname{sgn}(\lambda_2) \cdot \operatorname{sgn}(\sin x_9) \left\{ \operatorname{sgn} \left(\left| \lambda_2 \sin x_9 \right| - 2\bar{k}\alpha I_x \right) + 1 \right\} / 2 \quad .$$

This expression shows that \bar{u}_1 is a bang-bang type and has a dead zone. Figure 11 illustrates \bar{u}_1 vs. $(\lambda_2 \sin x_9 / 2\bar{k}\alpha I_x)$.



TA-7204-11

FIGURE 11 ILLUSTRATION OF \bar{u}_1

The width of the dead band is a function of the weighting factor \bar{k} . If \bar{k} is small, which corresponds to near time optimal, the dead band becomes narrow; the dead band becomes wider as \bar{k} increases. Roughly speaking, the minimum power control law \bar{u}_1 can be obtained by adding a dead zone to the switching curve for the minimum time control. A similar argument is true for \bar{u}_2 and is expressed as

$$\bar{u}_2 = -\alpha \operatorname{sgn}(\lambda_4) \operatorname{sgn}(\sin x_9) \left\{ \operatorname{sgn} \left(\left| \lambda_4 \sin x_9 \right| - 2\bar{k}\alpha I_y \right) + 1 \right\} / 2 .$$

F. Effects of Time Delay

For the CMG system considered here, a differential equation with time delay--or, more accurately, a differential-difference equation--may describe the system more realistically than an ordinary differential

equation. This is particularly true if the significant time delays exist in both the sensors and the control actuators. The former delay exists in the feedback loop of the system, and the latter delays exist in the control function.

It is the objective of this research to obtain a practical approximate solution rather than impractical exact solution. Hence the sub-optimal feedback control laws are found by using simplified equations of motion. As a result, the effect of time delays are neglected altogether.

G. Reduction of Model through Polar Coordinates
and Another Approach to Time-Optimal Control

The ten states of the optimal control problem formulated in Section III-B will now be transformed to other states using certain polar-coordinate and other transformations. The objective of optimization will be to drive certain states to zero in minimum time although the approach that follows could just as easily be applied to fuel optimization or a weighted combination of time and fuel. Beginning with the state dynamics equations (23), we define new coordinates by:

$$y_1 = \frac{I}{H} x_1 \quad y_2 = \frac{I}{H} x_2 \quad (45)$$

$$y_3 = \frac{I}{H} x_3 \quad y_4 = \frac{I}{H} x_4 \quad (46)$$

$$y_5 = \frac{I}{H} x_5 \quad y_6 = \frac{I}{H} x_6 \quad (47)$$

$$y_7 = x_7 \sin x_9 + x_8 \cos x_9 \quad (48)$$

$$y_8 = -x_7 \cos x_9 + x_8 \sin x_9 \quad (49)$$

$$y_9 = x_9 \quad y_{10} = x_{10} \quad . \quad (50)$$

Thus (y_7, y_8) is the vector (x_7, x_8) rotated counterclockwise through an angle $x_9 - \pi/2$, and the dimensions of y_7 and y_8 are in radians.

Using the data for I_x , I_y , and I_z given after Eq. (20) gives the dimensions of y_1 , y_3 , and y_5 as $\text{rad}\cdot\text{second}/\text{ft}^2$. Next, we define new controls v_1, v_2 by

$$v_1 = u_1 \sin x_9 + u_2 \cos x_9 \quad (51)$$

$$v_2 = u_1 \cos x_9 + u_2 \sin x_9 \quad . \quad (52)$$

Here again, (v_1, v_2) is (u_1, u_2) rotated through $x_9 - \pi/2$, and the dimensions of v_1 and v_2 are also in rad/second .

Now the state dynamics Eqs. (23) become

$$\dot{y}_1 = y_2 \quad (53)$$

$$\dot{y}_2 = y_{10}y_8 - v_1 \quad (54)$$

$$\dot{y}_3 = y_4 \quad (55)$$

$$\dot{y}_4 = -y_{10}y_7 - v_2 \quad (56)$$

$$\dot{y}_5 = y_6 \quad (57)$$

$$\begin{aligned} \dot{y}_6 &= x_7 u_1 + x_8 u_2 + \frac{I}{H} u_3 \\ &= y_7 v_1 + y_8 v_2 + \frac{I}{H} u_3 \end{aligned} \quad (58)$$

$$\begin{aligned}
\dot{y}_7 &= \dot{x}_7 \sin x_9 + \dot{x}_8 \cos x_9 + (x_7 \cos x_9 - x_8 \sin x_9) \dot{x}_9 \\
&= u_1 \sin x_9 + u_2 \cos x_9 - y_8 y_{10} \\
&= y_1 - y_8 y_{10}
\end{aligned} \tag{59}$$

$$\begin{aligned}
\dot{y}_8 &= -\dot{x}_7 \cos x_9 + \dot{x}_8 \sin x_9 + (x_7 \sin x_9 + x_8 \cos x_9) \dot{x}_9 \\
&= -u_1 \cos x_9 + u_2 \sin x_9 + y_7 y_{10} \\
&= y_2 + y_7 y_{10}
\end{aligned} \tag{60}$$

$$\dot{y}_9 = y_{10} \tag{61}$$

$$\dot{y}_{10} = u_3 \tag{62}$$

Equations (54), (56), (59), and (60) show that the problem is "uncontrollable" in the sense that y_1, \dots, y_8 (and hence x_1, \dots, x_8) cannot all be driven to zero by the controls u_1 and u_2 .

Notice also that now the equations no longer involve complicated terms such as $\sin y_9$ and $\cos y_9$, and that they are quadratic. In fact, since it is not desired to drive y_9 to zero, and y_9 now no longer appears on the right-hand side, it may be eliminated in finding optimal controls. However, it must be remembered that y_9 is needed to calculate the original variable x_1, \dots, x_8 in terms of y_1, \dots, y_8 once an optimal control is determined using the transformed system.

Next, we introduce polar coordinates by the relations:

$$y_1 = p \cos \varphi \quad y_2 = r \cos \Theta \tag{63}$$

$$y_3 = p \sin \varphi \quad y_4 = r \sin \Theta \tag{64}$$

$$y_7 = s \cos \sigma \quad y_8 = s \sin \sigma \tag{65}$$

Thus, we have

$$\Theta = \tan^{-1} \left(\frac{I_{y_4} x_4}{I_{x_2} x_2} \right)$$

$$\varphi = \tan^{-1} \left(\frac{I_{y_3} x_3}{I_{x_1} x_1} \right) .$$

Using Eqs. (63), (64), and (65), we can convert Eqs. (53) through (62) above to equations in the state variables Θ , φ , σ , r , p , s , y_9 , y_{10} , and control variables v_1 , v_2 , u_3 , by proceeding as follows:

$$\dot{p} \cos \varphi - p \dot{\varphi} \sin \varphi = r \cos \Theta \quad (66)$$

$$\dot{p} \cos \varphi + p \dot{\varphi} \cos \varphi = r \sin \Theta \quad (67)$$

$$\dot{r} \cos \Theta - r \dot{\Theta} \sin \Theta = y_{10} s \sin \sigma - v_1 \quad (68)$$

$$\dot{r} \sin \Theta + r \dot{\Theta} \cos \Theta = -y_{10} s \cos \sigma - v_2 \quad (69)$$

$$\dot{s} \cos \sigma - s \dot{\sigma} \sin \sigma = v_1 - s y_{10} \sin \sigma \quad (70)$$

$$\dot{s} \sin \sigma + s \dot{\sigma} \cos \sigma = v_2 + s y_{10} \cos \sigma . \quad (71)$$

Simplifying, we obtain

$$\dot{p} = r \cos (\Theta - \varphi) \quad (72)$$

$$\dot{r} = -v_1 \cos \Theta - v_2 \sin \Theta + y_{10} s \sin (\sigma - \Theta) \quad (73)$$

$$\dot{s} = v_1 \cos \sigma + v_2 \sin \sigma \quad (74)$$

$$p \dot{\varphi} = r \sin (\Theta - \varphi) \quad (75)$$

$$r \dot{\Theta} = -y_{10} s \cos (\sigma - \Theta) - v_2 \cos \Theta + v_1 \sin \Theta \quad (76)$$

$$s \dot{\sigma} = -v_1 \sin \sigma + v_2 \cos \sigma + s y_{10} . \quad (77)$$

It is noticed that one can let

$$\psi = \Theta - \varphi - \pi \quad * \quad (78)$$

$$w_1 = -v_1 \cos \Theta - v_2 \sin \Theta \quad (79)$$

$$w_2 = v_1 \sin \Theta - v_2 \cos \Theta \quad , \quad (80)$$

which enables further simplification. Note that Eqs. (79) and (80) merely rotate the control vector (u_1, u_2) [which has already been rotated once to form (v_1, v_2)] to form still another control vector (w_1, w_2) .

One then obtains

$$v_1 = -w_1 \cos \Theta + w_2 \sin \Theta \quad (81)$$

$$v_2 = -w_1 \sin \Theta - w_2 \cos \Theta \quad (82)$$

$$\dot{p} = r \cos \psi \quad (83)$$

$$\dot{r} = w_1 + y_{10}^s \sin (\sigma - \Theta) \quad . \quad (84)$$

Using Eqs. (81), (82), and (74), one obtains

$$\begin{aligned} \dot{\sigma} &= -w_1 (\cos \Theta \cos \sigma + \sin \Theta \sin \sigma) - w_2 (\cos \Theta \sin \sigma - \sin \Theta \cos \sigma) \\ &= -w_1 \cos (\sigma - \Theta) - w_2 \sin (\sigma - \Theta) \quad . \end{aligned} \quad (85)$$

It now becomes clear that σ and Θ can be replaced by ψ and η , where ψ is as in Eq. (78) and

$$\eta = \sigma - \Theta - \pi \quad , \quad (86)$$

(the π appears here for a special reason, as will be explained later).

This leads to the following:

$$\dot{p} = -r \cos \psi \quad (87)$$

$$\dot{r} = w_1 - y_{10}^s \sin \eta \quad (88)$$

$$\dot{\sigma} = w_2 \sin \eta + w_1 \cos \eta \quad (89)$$

* The π appears here because $\Theta - \varphi = \pi$ in the terminal phase of control using our approach in the Appendix; i.e., the velocity vector is opposite to the position vector near the origin in $\theta_x - \theta_y$ space.

$$\dot{y}_5 = y_6 \quad (90)$$

$$\begin{aligned} \dot{y}_6 &= Lu_3 + x_7 u_1 + x_8 u_2 \\ &= Lu_3 + (x_7, x_8) \cdot (u_1, u_2) \\ &= Lu_3 + (y_7, y_8) \cdot (v_1, v_2) \quad , \end{aligned}$$

where $L = I/H$. The last line follows from the fact that both the states and controls here have been rotated through the same angle $x_9 - \pi/2$.

But from Eqs. (74) and (65), we also note that

$$\begin{aligned} s\dot{s} &= s(v_1 \cos \sigma + v_2 \sin \sigma) \\ &= (y_7, y_8) \cdot (v_1, v_2) \quad . \end{aligned}$$

Thus, we have

$$\dot{y}_6 = Lu_3 + s\dot{s} \quad (91)$$

or, in other terms,

$$\dot{y}_6 = Lu_3 + s(w_2 \sin \eta + w_1 \cos \eta) \quad . \quad (91')$$

Continuing for the remaining states, we have

$$\dot{\psi} = \Theta - \dot{\phi} = \frac{y_{10}s}{r} \cos \eta + \frac{w_2}{r} + \frac{r}{p} \sin \psi \quad (92)$$

$$\begin{aligned} \dot{\eta} = \dot{\sigma} - \Theta &= -\left(\frac{v_1 \sin \sigma - v_2 \cos \sigma}{s}\right) + y_{10} - y_{10} \frac{s}{r} \cos \eta \\ &\quad -\left(\frac{v_1 \sin \theta - v_2 \cos \theta}{s}\right) \\ &= y_{10} \left(1 - \frac{s}{r} \cos \eta\right) + \left(\frac{-w_1 \sin \eta + w_2 \cos \eta}{s}\right) - \frac{w_2}{r} \quad , \quad (93) \end{aligned}$$

after simplifying by using Eqs. (81), (82), and (86).

Finally, we still have

$$\dot{y}_9 = y_{10} \quad (94)$$

$$\dot{y}_{10} = u_3 \quad (95)$$

The reason for choosing $\eta = \sigma - \Theta - \pi$ above is that η remains equal to 0 and r remains equal to s when

- (1) $\eta = 0$ and $r = s$ prior to any θ_x or θ_y disturbances and
- (2) There are negligible external disturbances on the θ_z axis of the space vehicle.

Prior to any θ_x or θ_y disturbances, we have the following situation:

- (1) The initial conditions $\theta_x = \theta_y = 0$ imply that $p = r = 0$,
- (2) $s = 0$ since no control torques are being developed and s is the magnitude of the vector (θ_1, θ_2) , which represents angular displacements at the two inner gimbals,
- (3) Since both vectors $(\dot{\theta}_x, \dot{\theta}_y)$ and (θ_1, θ_2) are of zero length, their angles Θ , σ , and thus η are all ambiguous; thus one may arbitrarily assign η the value 0 initially.

Once disturbances occur on the θ_x and θ_y axes, the magnitude r of the vector $(\dot{\theta}_x, \dot{\theta}_y)$ assumes a positive value, and Θ assumes a well-defined value. But the instant this happens, the vector (θ_1, θ_2) is displaced from $(0, 0)$ also, leading to a well-defined value of σ and a positive value of s . The important fact, however, is that (θ_1, θ_2) is displaced in such a way that η and $r - s$ remain equal to zero when they are 0 initially. To demonstrate this fact, let $\eta = r - s = 0$ in Eqs. (87)-(95). This leads to

$$\dot{\eta} = y_{10} (1 - 1) + \frac{w_2}{r} - \frac{w_2}{r} = 0 \quad (96)$$

$$\dot{\psi} = \frac{w_2}{r} + \frac{r}{p} \sin \psi + y_{10} \quad (97)$$

$$\dot{r} = w_1 \quad (98)$$

$$\dot{s} = w_1 \quad (99)$$

$$\dot{p} = -r \cos \psi \quad (100)$$

$$\dot{y}_9 = y_{10} \quad , \quad \dot{y}_{10} = u_3 \quad . \quad (101)$$

Since it is now assumed there are no z-axis external disturbances, to maintain $y_6 = y_5 = 0$, we must counteract the effect of $s\dot{s}$ in Eq. (91) so that

$$\dot{y}_6 = Lu_3 + s\dot{s} = 0 \quad , \quad (102)$$

i.e.,

$$u_3 = -\frac{s\dot{s}}{L} = 2Ks\dot{s} \quad , \quad (103)$$

where $K = -1/2L$. Equation (103) yields the same value for u_3 as Eq. (26). We assume that this counter torque is physically achievable with negligible time delay compared to the damped oscillation periods of the order of about 1 second for the differential equation system (97), (98), and (100) combined with the feedback control law of Table A-1, in the Appendix, as observed in Figures 15 and 17.

From Eqs. (96), (98), and (99), it follows that $\eta = 0$, $r = s$ will be maintained when $\dot{\eta} = 0$, and $r = s$ initially. Furthermore, Eqs. (101), (102), and (103) imply

$$Ks^2 = Kr^2 = y_{10} + C \quad , \quad (104)$$

where $C = C(t)$, and depends upon external forces acting on the z axis of the space vehicle, which leads to an additional reaction torque for the control u_3 different from the value given by Eq. (103). $C(t)$ is the time integral of any external disturbance torques on the z axis. Assuming that these disturbance torques are small compared with the torque u_3 produced by Eq. (102) to keep the space vehicle fixed about the θ_z axis, we can set $C = 0$. Combining Eq. (104) with Eqs. (97) through (100), we obtain

$$\dot{s} = \dot{r} = w_1 \quad (105)$$

$$\dot{p} = -r \cos \psi \quad (106)$$

$$\dot{\psi} = \frac{w_2}{r} + \frac{r}{p} \sin \psi + Kr^2 \quad . \quad (107)$$

These are the equations of the reduced problem solved in the Appendix.

We will now show what happens to s and η when p , r , and ψ have been driven to 0 (i.e., if the five-state problem of the Appendix is solved) without requiring that $r \equiv s$ and $\eta \equiv 0$.

From Eqs. (87), (88), and (92), we see that once p , r , and ψ are 0, then they are maintained at 0 by keeping the controls w_1 and w_2 equal to

$$w_1 = y_{10} s \sin \eta \quad (108)$$

$$w_2 = -y_{10} s \cos \eta \quad . \quad (109)$$

Substituting this in Eq. (93), we see that

$$\dot{\eta} = y_{10} \left(1 - \frac{s}{r} \cos \eta \right) - \frac{y_{10} s}{s} + \frac{y_{10} s \cos \eta}{r} = 0 \quad .$$

Actually there is some degeneracy in this formula as $r \rightarrow 0$, but clearly in any practical situation r is never really 0; thus $\dot{\eta}$ is in fact 0, since the terms $s/r \cos \eta$ cancel one another when w_2 is maintained at the value $-y_{10} s \cos \eta$.

Substituting in Eq. (89), we see that

$$\dot{s} = y_{10} s \sin \eta \cos \eta - y_{10} s \cos \eta \sin \eta = 0 \quad .$$

Hence s can never be driven to zero once r , p , and ψ are 0. The physical interpretation of this is that one cannot drive the gimbal deviations θ_1 and θ_2 to zero once one is finished with driving the deviations θ_x , θ_y , θ_z , $\dot{\theta}_x$, $\dot{\theta}_y$, and $\dot{\theta}_z$ to zero. Theoretically, simultaneous control of $\dot{\theta}_1$, $\dot{\theta}_2$ and $\ddot{\theta}_3$ to drive r , p , s , y_5 , and y_6 to zero is possible by taking advantage of the higher order terms that were neglected to arrive at Eqs. (19). However, because of the fact that such control would be based on using high-order terms involving θ_1 and θ_2 in the range $|\theta_i| \leq 0.07$ radian, it is expected to be too inefficient; i.e., a great deal of oscillating back and forth around the origin in r - p space would be needed while s is slowly being driven to zero. To justify this claim, consider the assumptions regarding the smallness of θ_1 and θ_2 that were made before Eqs. (12). Now, if one backs up a step from that stage, one can write

$$T_1 = -H \left(\dot{\theta}_2 \cos \theta_1 + \dot{\theta}_3 \sin \theta_1 \cos \theta_2 \right) \quad (110)$$

$$T_2 = H \cos \theta_1 (\dot{\theta}_1 - \dot{\theta}_3 \sin \theta_2) \quad (111)$$

$$\begin{aligned} T_3 &= H \sin \theta_2 (\dot{\theta}_2 \cos \theta_1 + \dot{\theta}_3 \sin \theta_1 \cos \theta_2) \\ &\quad + H \sin \theta_1 \cos \theta_2 (\dot{\theta}_1 - \dot{\theta}_3 \sin \theta_2) + I\ddot{\theta}_3 \\ &= H \cos \theta_2 (\sin \theta_1 \dot{\theta}_1 + \sin \theta_2 \dot{\theta}_2) + I\ddot{\theta}_3 \end{aligned} \quad (112)$$

in place of Eqs. (19). These clearly reduce to the latter when θ_1 and θ_2 are small. The result of using the more exact equations (110), (111), and (112) is as follows (we omit the details of derivation): Equations (54), (56), (59), and (60) are to be replaced by

$$\dot{y}_2 = y_{10}y_8 - v_1 \cos \theta_1$$

$$\dot{y}_4 = -y_{10}y_7 - v_2 \cos \theta_1$$

$$\dot{y}_7 = v_1 \cos \theta_1 \cos \theta_2 - y_{10}y_8$$

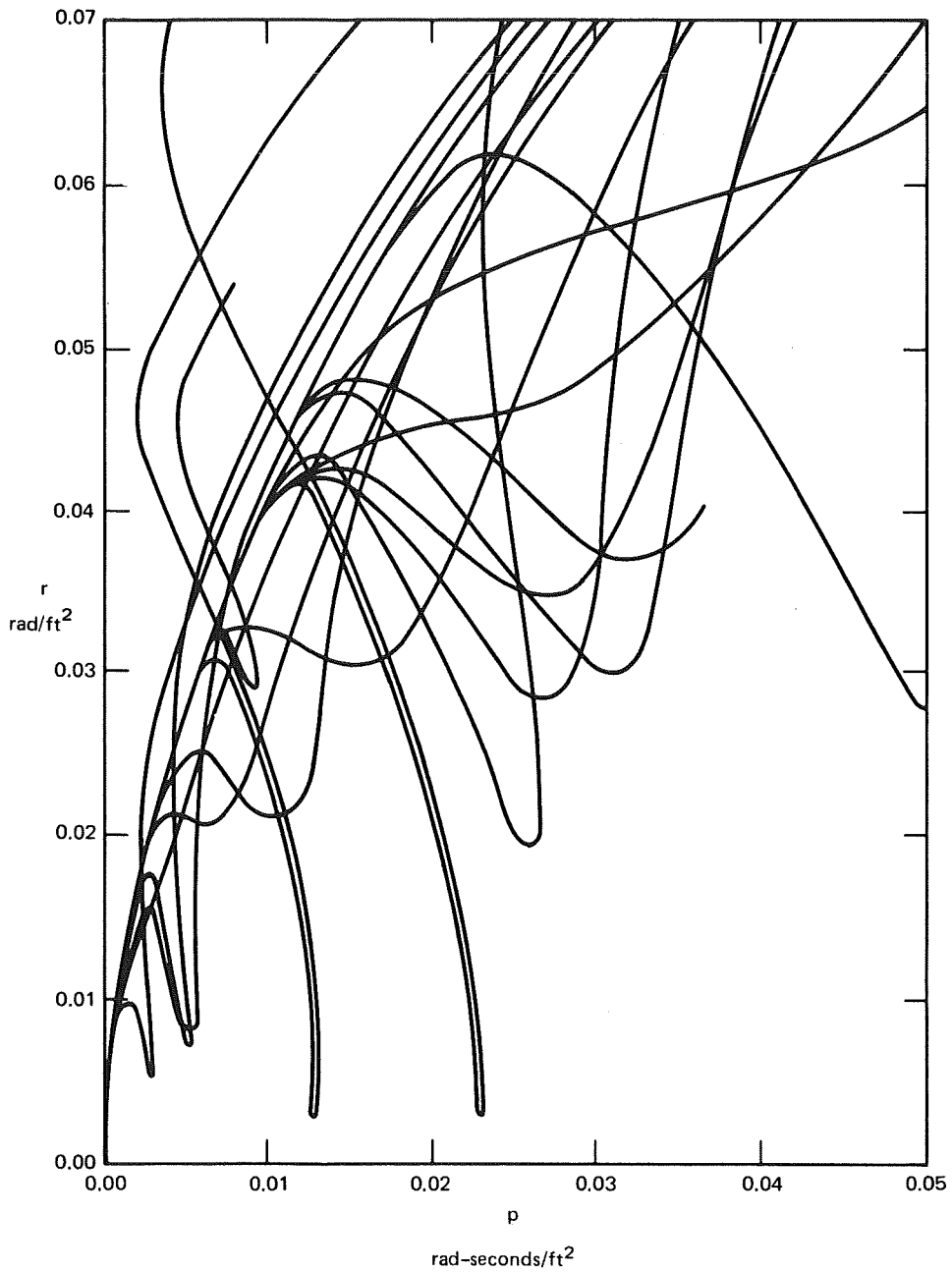
$$\dot{y}_8 = v_2 \cos \theta_1 \cos \theta_2 + y_{10}y_7$$

Now \dot{y}_7 and \dot{y}_8 differ from $-\dot{y}_2$ and $-\dot{y}_4$ to a degree dependent upon the size of θ_1 and θ_2 . Hence it becomes technically possible to control (y_2, y_4) separately from (y_7, y_8) , but as $(y_7, y_8) \rightarrow 0$ [hence $(\theta_1, \theta_2) \rightarrow 0$] this difference diminishes as the square of θ_2 , since $\cos \theta_2 \approx 1 - \theta_2^2/2$. It can be easily checked that this implies infinite time to drive θ_1 and θ_2 to zero. Thus driving both the vehicle angular velocities and the gimbal deviations to zero does not appear practically feasible.

As was shown above, when $\eta = 0$, $r = s$, and $y_5 = y_6 = 0$, equations are obtained for which a reasonable suboptimal control law, a control law for the full eight-state problem consisting of Eqs. (87)-(93), and (95) is derivable, from which, in turn, one can control the original ten-state problem. This is achieved as follows: First, a feedback control law driving the first four states y_1, \dots, y_4 (hence the original $\theta_x, \dot{\theta}_x, \theta_y, \dot{\theta}_y$) to zero in close to minimum time is obtained, as described in the Appendix. This control law is then heuristically extended to the case with the states y_7 and y_8 included (although not being driven to zero), as shown in the Appendix. Then this can be combined with the well-known bang-bang time-optimal control law* for driving the states y_5 and y_6 to zero in the two-dimensional "regulator" problem whose state dynamics are given by Eqs. (57) and (58), treating all but y_5, y_6 , and u_3 as external disturbances. The above procedure is tantamount to decoupling the original ten-state problem into the two independent time-optimal control problems obtained by using only the eight states $y_1, \dots, y_4, y_7, \dots, y_{10}$ in one and the states y_5 and y_6 in the other. This decoupling is justified with respect to the effect of the two-state problem upon the eight-state problem because the states y_5 and y_6 do not enter in the equations of the other states. However, the effect of the eight-state problem upon the two-state problem above is quite strong. In Eq. (91) the term $(y_7, y_8) \cdot (v_1, v_2)$ is bounded by $s \times 0.0872 \leq 0.006$, since $|s| = y_7^2 + y_8^2 \leq 0.07$, based on maximum expected 1st and 2nd gimbal deviations of $0.05 \text{ rad} \cong 3^\circ$, in accordance with Section IV-D, while the term Lu_3 in Eq. (91) takes on the values $\pm 13/1000 \ 0.1745 \cong 0.002$, using the data given after Eq. (15) in Sections II-B and IV-C. Thus the "disturbance" term in Eq. (91) may override the control torque term and prevent driving $y_5 = \theta_z$ and $y_6 = \dot{\theta}_z$ to zero

* See Ref. 3.

using the outer gimbal under worst-case deviations of the inner gimbals (θ_1, θ_2) considered in this report. For larger outer gimbal and for smaller expected deviations of θ_1 and θ_2 , however, the decoupling would be justified with respect to the effect of s upon \dot{y}_6 . The control law derived here on the basis of decoupling has been tested so far only on a reduced version of the eight-state problem having only the five states $\theta_x, \dot{\theta}_x, \theta_y, \dot{\theta}_y,$ and $\dot{\theta}_3$. The results for this reduced problem are shown in Figures 12-17. Further testing using the entire decoupled ten-state problem would be required to justify the above approach satisfactorily. The scales for $p, z,$ and z_3 in Figures 12-17 are in units of rad-second/ ft^2 , and for r the scale is in rad/ ft^2 . Using the values of I_x and I_y after Eq. (20), and the value of H after Eq. (15), and referring to Eqs. (45)-(47), these scales should be divided by 40 to obtain the length of the vector (θ_x, θ_y) and its derivative in radians and rad/second. Thus the maximum value of 0.05 for p in Figures 12 and 13 corresponds to a maximum deviation of 0.00125 rad for the vector (θ_x, θ_y) , which corresponds approximately to the maximum deviation of 0.00075 rad assumed for θ_x and θ_y in Section IV-D.



TA-7204-12

FIGURE 12 OPTIMAL TRAJECTORIES IN p - r - ψ SPACE PROJECTED ONTO THE p - r PLANE

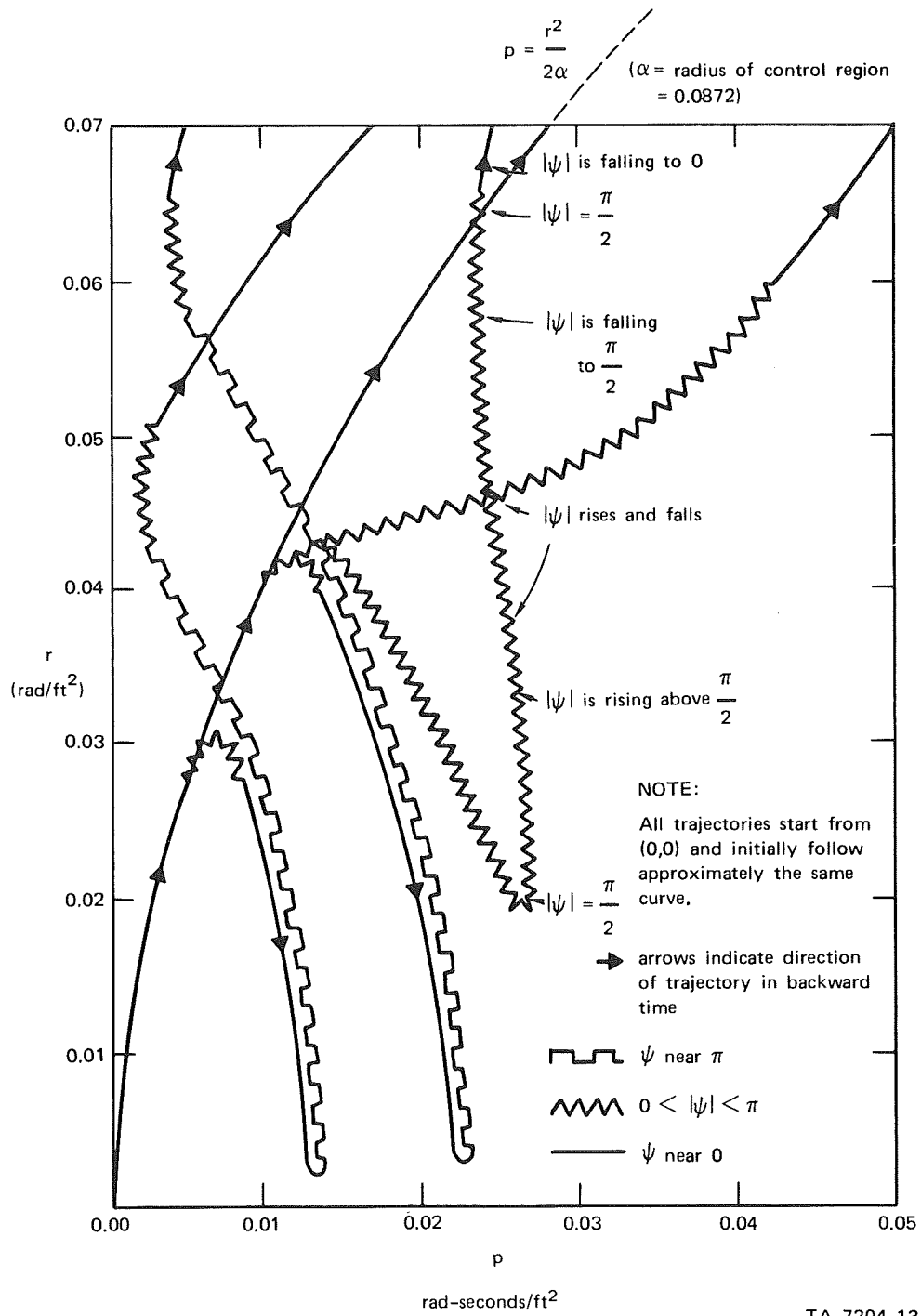


FIGURE 13 THE PATTERN OF OPTIMAL TRAJECTORIES IN p - r - ψ SPACE PROJECTED ONTO THE p - r PLANE

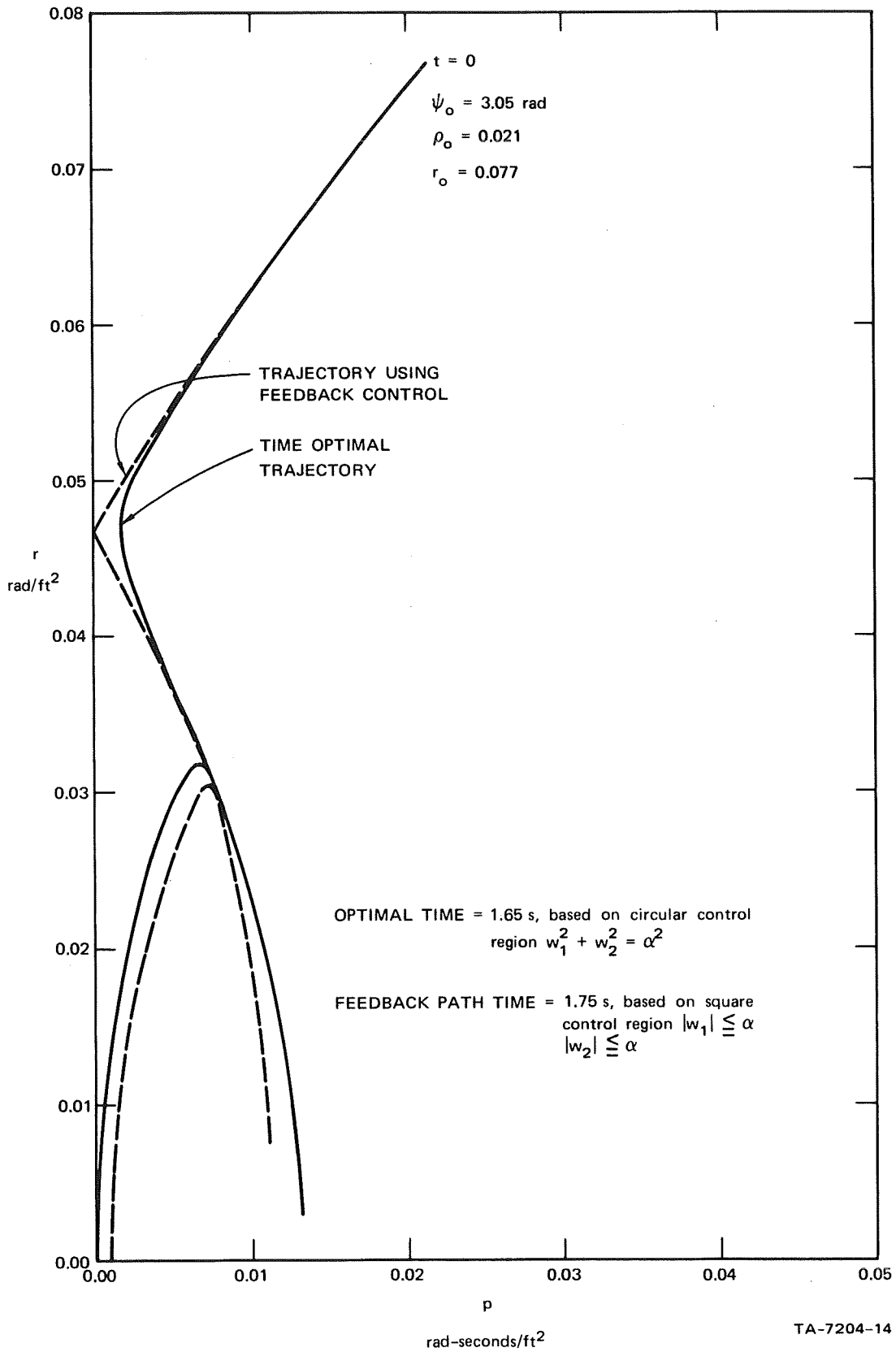
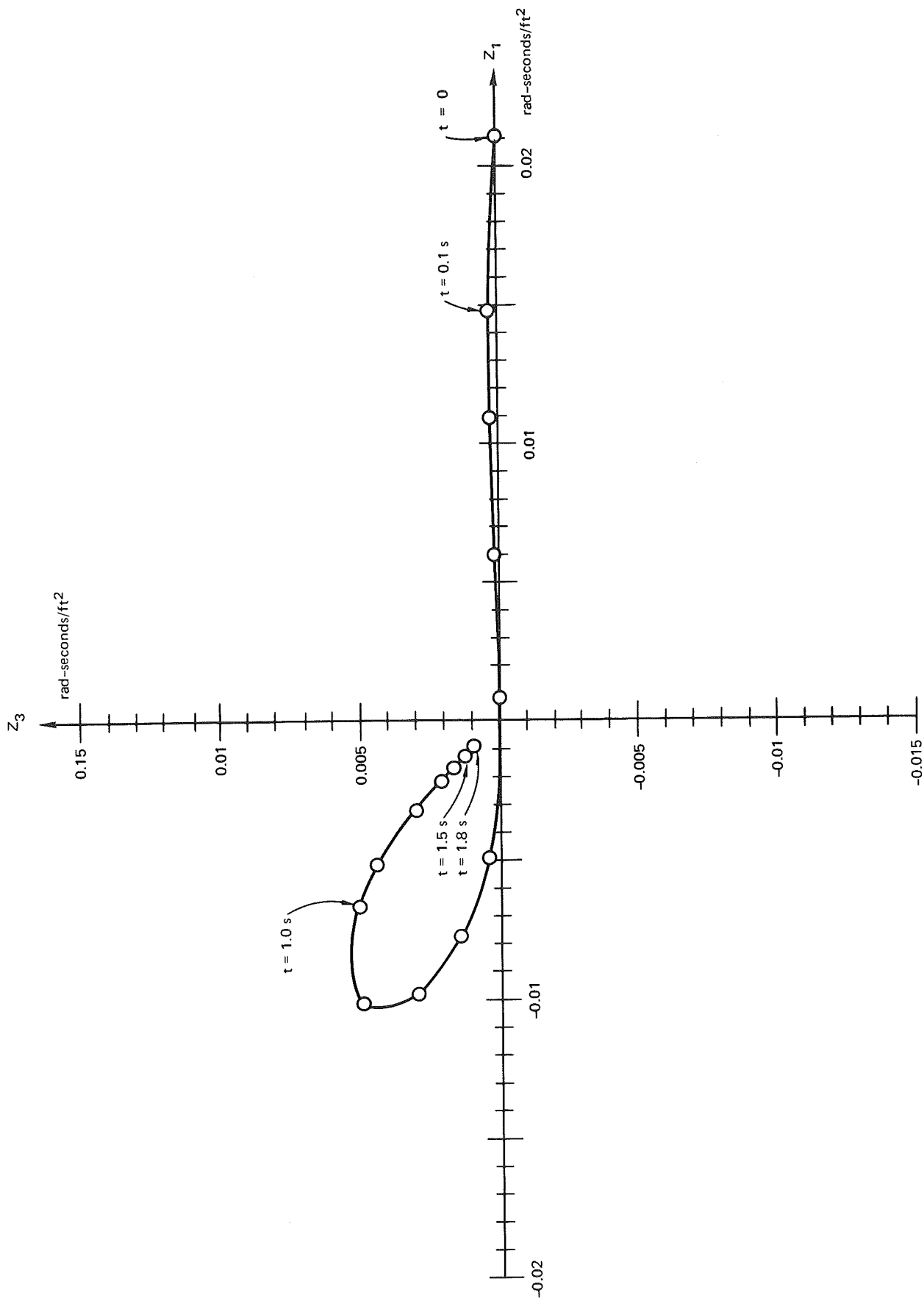


FIGURE 14 COMPARISON OF OPTIMAL AND FEEDBACK TRAJECTORIES IN p-r PLANE FOR INITIAL POINT A



TA-7204-15

FIGURE 15 FEEDBACK TRAJECTORY IN Z_1 - Z_3 PLANE FOR INITIAL POINT A

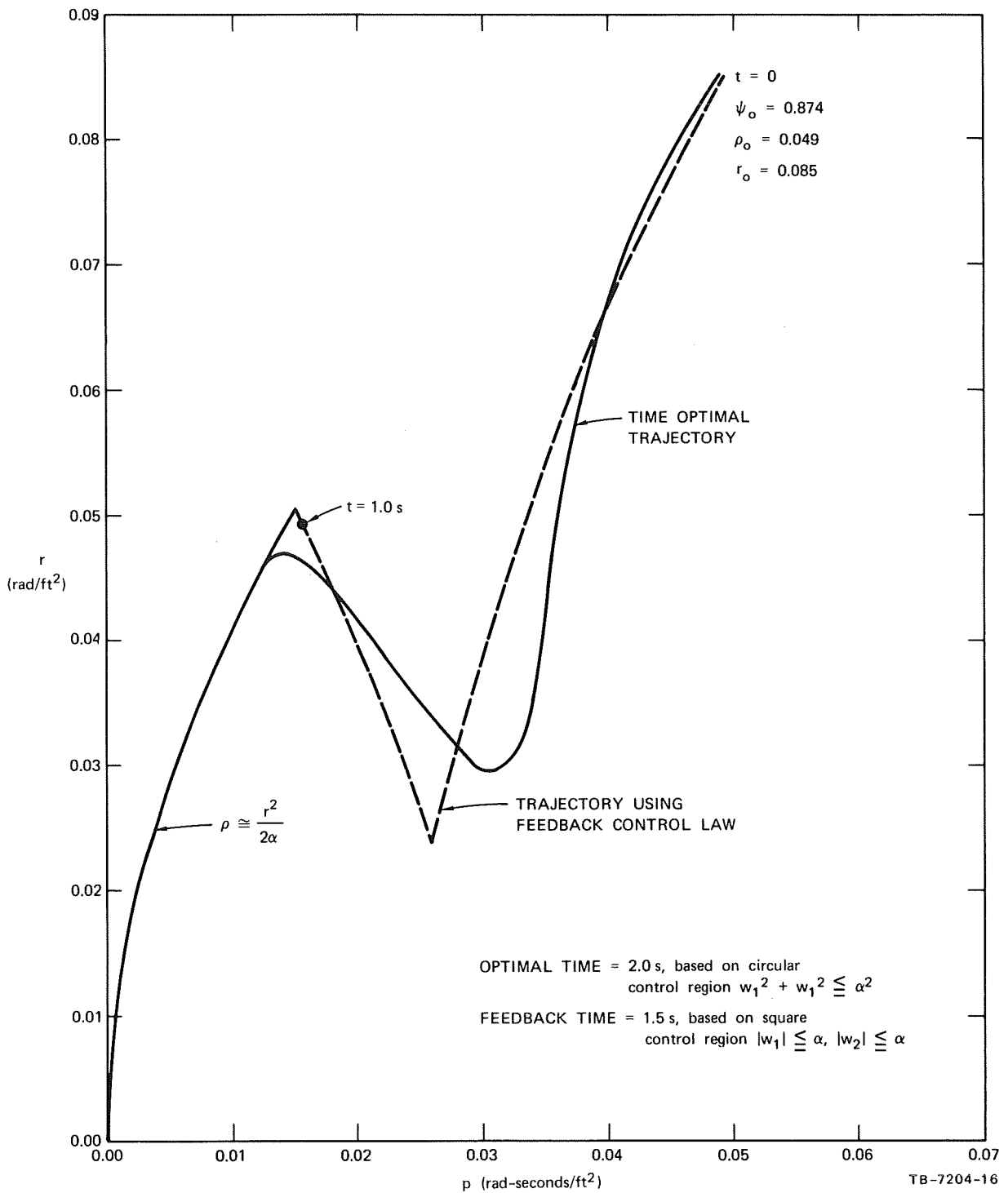


FIGURE 16 COMPARISON OF OPTIMAL AND FEEDBACK TRAJECTORIES IN p-r PLANE FOR INITIAL POINT B

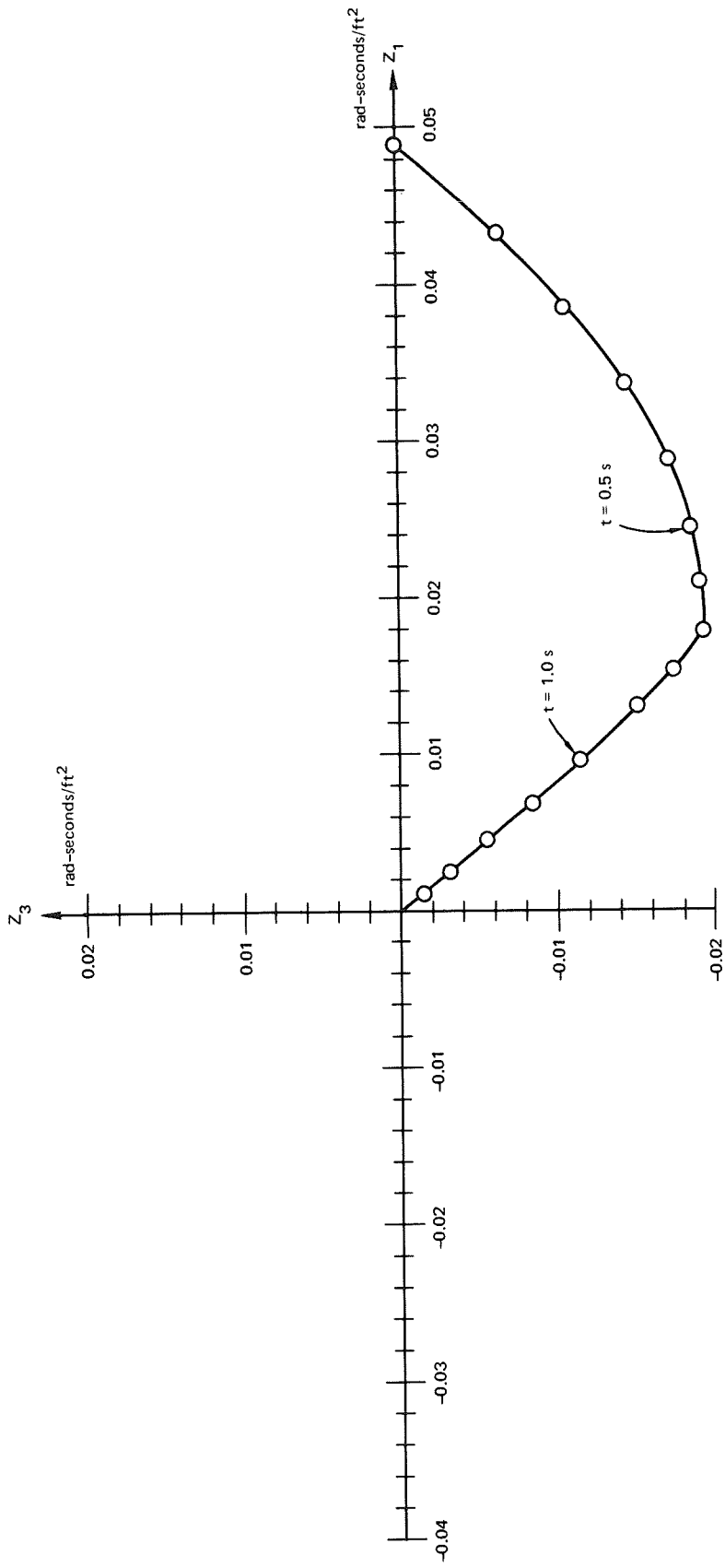


FIGURE 17 FEEDBACK TRAJECTORY IN $Z_1 - Z_3$ PLANE FOR INITIAL POINT B

TA-7204-17

V CONCLUSION

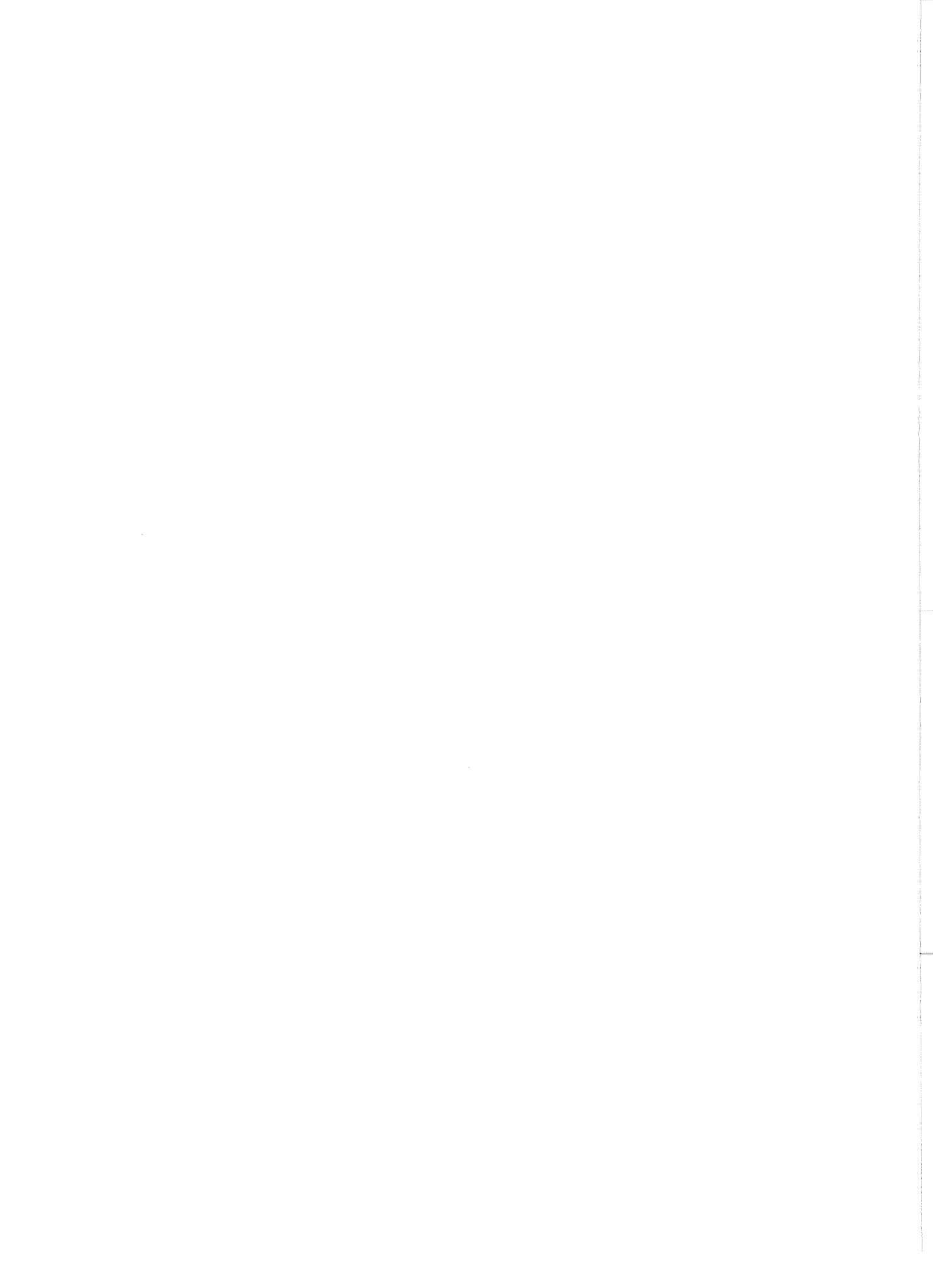
A theoretical study has been made for a single three-gimbaled control moment gyro. In order to obtain a feasible feedback control law, the equations of motion were simplified. The suboptimal control derived for the simplified equations performed very well for the small disturbances. For testing purposes, the feedback suboptimal control law for minimum time was applied to several different cases.

It was found that the outer gimbal with the present configuration is not suitable for controlling the disturbances about the z axis. However, the outer gimbal is necessary in the present form to permit adequate x and y axis control.

The optimal control law that minimizes both time and power with a weighting factor was constructed by adding a dead zone to the time-optimal switching curves. The width of the dead band is a function of the weighting factor.

The time-optimal control problem presented in Section IV-G is considered from a different point of view. The time-optimal control laws are derived in a heuristic manner and the simplicity of the resulting control laws is the significance of this approach.

Since this report is the result of the initial phase study, many improvements and detailed investigation in some parts are required.



APPENDIX

DERIVATION OF FEEDBACK CONTROL FOR THREE-DIMENSIONAL SYSTEM

A feedback control for the reduced system of equations (105)-(107) will be described here. It will then be shown how this control law extends to the case of Eqs. (87)-(95) when it is assumed, just as for Eqs. (105)-(107), that no external disturbances to y_5 and y_6 occur, i.e., when Eqs. (102) and (103) can be assumed. Hence, as discussed at the end of Section IV-G, a control law for the original problem, as formulated by Eqs. (53)-(62), will be obtainable by simple transformation of coordinates and superposition of the two control laws of the decoupled systems.

Returning to the problem of Eqs. (105)-(107), let us write down the conditions of the maximum principle and the adjoint equation not for this problem but for a problem one step back of this in our derivation, namely, the one given by returning from polar to rectangular coordinates; i.e., interpret (p, σ) and (r, Θ) again as vectors (z_1, z_3) and (z_2, z_4) and ψ as $\Theta - \sigma - \pi$. This will lead to equations of the form

$$\dot{z}_1 = z_2 \tag{A-1}$$

$$\dot{z}_2 = K \left(z_2^2 + z_4^2 \right) z_4 - v_1 \tag{A-2}$$

$$\dot{z}_3 = z_4 \tag{A-3}$$

$$\dot{z}_4 = -K \left(z_2^2 + z_4^2 \right) z_2 - v_2 \tag{A-4}$$

in four state variables z_1, \dots, z_4 , if v_1 and v_2 are related to w_1 and w_2 as in Eqs. (79) and (80). Because of the assumptions made in arriving at Eqs. (105)-(107), z_1, \dots, z_4 are not exactly equal to y_1, \dots, y_4 , unless the constant C in Eq. (104) is 0, etc. However, under those assumptions, z_1, \dots, z_4 represent the original gimbal deviations and gimbal rates multiplied by certain constant factors. The reason for going back to a four-state rectangular problem is computational convenience; this problem was synthesized by the maximum principle on a time-sharing teletype computer and it was found that better accuracy and speed with simple Euler integration could be achieved by avoiding the highly nonlinear terms in Eqs. (105)-(107) compared with the simpler cubic terms in Eqs. (A-2) and (A-4). Furthermore, since the two problems are equivalent, the four-state problem needed to have only three of its adjoint variables swept over suitable ranges in using the maximum principle instead of four, as would be necessary for a general problem of dimension 4, and therefore the simulation effort was not actually increased by elevating the state dimension from three to four.

The adjoint equations are

$$\dot{\lambda}_1 = 0 \quad (\text{A-5})$$

$$\dot{\lambda}_2 = -\lambda_1 - 2Kz_2z_4\lambda_2 + K(3z_2^2 + z_4^2)\lambda_4 \quad (\text{A-6})$$

$$\dot{\lambda}_3 = 0 \quad (\text{A-7})$$

$$\dot{\lambda}_4 = -\lambda_2 - K\left(\frac{2}{z_2} + 3z_4^2\right)\lambda_2 + 2Kz_2z_4\lambda_4 \quad (\text{A-8})$$

The Hamiltonian, to be maximized, is

$$\mathcal{H} = \lambda_1 z_1 + \lambda_3 z_3 + \lambda_2 \left[K \left(z_2^2 + z_4^2 \right) z_4 - v_1 \right] - \lambda_4 \left[K \left(z_2^2 + z_4^2 \right) z_2 - v_2 \right] \quad . \quad (\text{A-9})$$

The maximum is achieved at

$$v_1 = \frac{-\alpha \lambda_2}{\sqrt{\lambda_2^2 + \lambda_4^2}} \quad (\text{A-10})$$

$$v_2 = \frac{\alpha \lambda_4}{\sqrt{\lambda_2^2 + \lambda_4^2}} \quad (\text{A-11})$$

when using the circular control region $v_1^2 + v_2^2 \leq \alpha^2$, or at

$$v_1 = -\alpha \operatorname{sign}(\lambda_2)$$

$$v_2 = \alpha \operatorname{sign}(\lambda_4)$$

when using the square control region $|w_1| \leq \alpha$, $|w_2| \leq \alpha$. The latter was used in deriving Figures 14-17, while the former was used to obtain Figures 12 and 13. Which of these two is the easiest to incorporate into a usable feedback control law remains to be determined. Here α was taken to be 0.0872, the magnitude of the original control vector (u_1, u_2) . The boundary conditions are

$$\lambda_i(0) \text{ free} \quad \lambda_i(T) \text{ free} \quad , \quad i = 1, 2, 3, 4 \quad ,$$

where T is the final time, for any fixed initial point $z_1(0), \dots, z_4(0)$. The terminal point is always to be $z_1(T) = \dots = z_4(T) = 0$, since we want to drive r and p to zero in the problem of Eqs. (105)-(107). Computing backward trajectories from the origin in z_1, \dots, z_4 space for different starting values for the λ_i 's resulted in curves in p - r space as shown in Figures 12 and 13. On the basis of these figures,

and the plotted values of ψ along the curves in these figures, a feedback control was heuristically arrived at, as given in Table A-1. Note that the switching value $\psi = \pm\pi/6$ instead of $\pm\pi/2$ was found to work

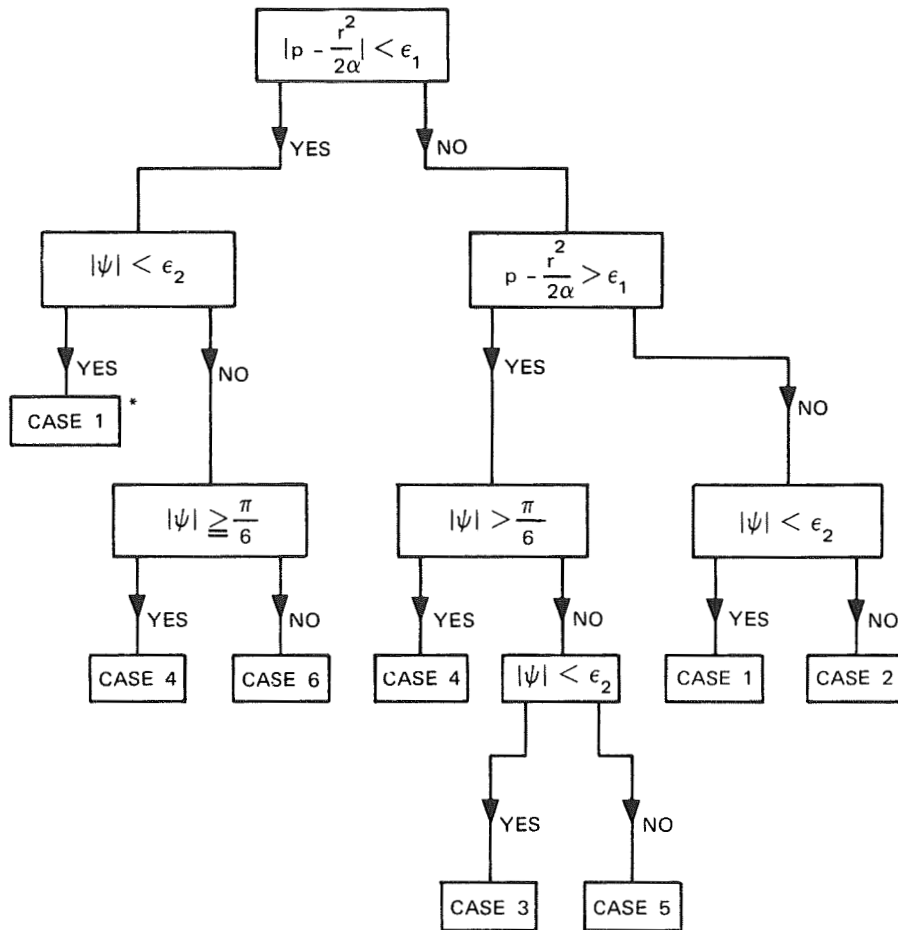
Table A-1

A PROVISIONAL SUBOPTIMAL FEEDBACK CONTROL LAW

(no dead bands)

| Case | w_1 | w_2 |
|--|---------------------|------------------------------------|
| 1. $p \leq r^2/2\alpha$ $\psi = 0$ | $-\alpha$ | $-Kr^3$ |
| 2. $p < r^2/2\alpha$ $\psi \neq 0$ | $-\alpha$ | $-\alpha \operatorname{sgn}(\psi)$ |
| 3. $p > r^2/2\alpha$ $\psi = 0$ | α | $-Kr^3$ |
| 4. $p \geq r^2/2\alpha$ $ \psi \geq \pi/2$ | $-\alpha$ | $-\alpha \operatorname{sgn}(\psi)$ |
| 5. $p > r^2/2\alpha$ $0 < \psi < \pi/2$ | α | $-\alpha \operatorname{sgn}(\psi)$ |
| 6. $p = r^2/2\alpha$ $0 < \psi < \pi/2$ | $-\alpha \cos \psi$ | $-\alpha \operatorname{sgn}(\psi)$ |

more efficiently and was used in the flow chart in Figure A-1. This control law, modified as in Figure A-1 was fed back into Eqs. (A-1)-(A-4) to see how well it represents the time-optimal policy for these equations. The results were reasonably good, and are shown for two starting points in z_1 - z_4 space [hence in p - r - ψ space for Eqs. (105)-(107)], in Figures 14-17. For computational convenience, the feedback law used to derive Figures 14-17 was the bang-bang control law of Figure A-1, which arose from using the square control region $|w_1| \leq \alpha$, $|w_2| \leq \alpha$,



* Cases refer to Table A-1.

TA-7204-18

FIGURE A-1 FLOW CHART USED FOR OBTAINING FIGURES 14-17

whereas Figures 12 and 13 were obtained using the circular control region given by $w_1^2 + w_2^2 \leq \alpha^2$; this explains the "optimal" time being greater than the feedback time in Figure 15. Actually, the shape of the feedback control region is rather arbitrary, since the controls w_1 and w_2 are not "physical" torques but rather result from rotation of the physical torque vector $(\dot{\theta}_1, \dot{\theta}_2)$ through a certain angle, and it is the latter vector that is physically constrained. For this reason, it seems best to use the circular region, since then $(\dot{\theta}_1, \dot{\theta}_2)$ would also be constrained to a circle.

The system (105)-(107) was obtained from Eqs. (87)-(95) by assuming $r = s$ and $\eta = 0$ and no external disturbances on the z axis. In the more general case where $r \neq s$ and $\eta \neq 0$, and there may be z-axis external disturbances there are more state variables to be considered. For this case, we have Eqs. (87), (88), (89), (92), (93), (95) for the states $p, r, \psi, \eta, s, y_{10}$. The control law of Table A-1 can be extended to this case heuristically by realizing that the term Kr^2 in Eq. (107) is really $y_{10} s/r \cos \eta$ in Eq. (92), and by noting that the states y_{10}, s, η are not being driven to zero. Thus the feedback control to drive p, r to zero should have $w_2 = -y_{10} s \cos \eta$ to keep $\dot{\psi} = 0$ when ψ reaches 0 in Eq. (92), instead of having $w_2 = -Kr^3$ in Eq. (107) as is stated in Case 1 of Table A-1. Treating the other cases of Table A-1 similarly results in Table A-2 for this more general problem.

This policy assumes that the term $w_1 = \pm\alpha$ can exceed the maximum magnitude $y_{10}s$ of the "disturbance" term in Eq. (88), and therefore, p and r are controllable through w_1 . As we pointed out in Section IV-G, this may not be possible, using the gimbal sizes and their maximum deviations assumed in this report. Also, so far it has been assumed that z-axis disturbance torques are negligible compared with the reaction torque u_3 that results in Eq. (102) to keep $\dot{y}_6 = I_z/H \dot{\theta}_z$ from being

Table A-2

SUGGESTED FEEDBACK CONTROL FOR USE WITH
EQS. (87), (88), AND (92) WHEN $r \neq s$ AND $\eta \neq 0$

| Case | w_1 | w_2 |
|--|--|-------------------------------------|
| 1. $p \leq r^2/2\alpha$ $\psi = 0$ | $-\alpha$ | $-y_{10}^s \cos \eta$ |
| 2. $p < r^2/2\alpha$ $\psi \neq 0$ | $-\alpha$ | $-\alpha \operatorname{sgn} \psi$ |
| 3. $p > r^2/2\alpha$ $\psi = 0$ | α | $-y_{10}^s \cos \eta$ |
| 4. $p \geq r^2/2\alpha$ $ \psi \geq \pi/2$ | $-\alpha$ | $-\alpha \operatorname{sgn} (\psi)$ |
| 5. $p > r^2/2\alpha$ $0 < \psi < \pi/2$ | α | $-\alpha \operatorname{sgn} (\psi)$ |
| 6. $p = r^2/2\alpha$ $0 < \psi < \pi/2$ | $-\alpha \cos \psi + y_{10}^s \sin \eta$ | $-\alpha \operatorname{sgn} (\psi)$ |

affected by motion of the inner gimbals. When there are larger z-axis disturbances, the assumptions leading to Eqs. (105)-(107) are not valid, and the control law of Table A-2 needs further testing under these conditions.



REFERENCES

1. P. R. Kurzhals and C. Grantham, "A System for Inertial Experiment Pointing and Attitude Control," NASA Technical Report, R-247 (August 1966).
2. T. R. Kane, Analytical Elements of Mechanics (Academic Press, 1961).
3. L. S. Pontryagin et al., The Mathematical Theory of Optimal Processes (John Wiley and Sons, 1962).
4. N. Kryloff and N. Bogoliuboff, Introduction to Nonlinear Mechanics (Princeton University Press, 1947).